Applications of a tight-binding total energy method for transition and noble metals: Elastic Constants, Vacancies, and Surfaces of Monatomic Metals

Michael J. Mehl and Dimitrios A. Papaconstantopoulos

Complex Systems Theory Branch, Naval Research Laboratory, Washington, D.C. 20375-5345

(February 8, 2008)

A recent tight-binding scheme provides a method for extending the results of first principles calculations to regimes involving $10^2 - 10^3$ atoms in a unit cell. The method uses an analytic set of two-center, non-orthogonal tight-binding parameters, on-site terms which change with the local environment, and no pair potential. The free parameters in this method are chosen to simultaneously fit band structures and total energies from a set of first-principles calculations for monatomic fcc and bcc crystals. To check the accuracy of this method we evaluate structural energy differences, elastic constants, vacancy formation energies, and surface energies, comparing to first-principles calculations and experiment. In most cases there is good agreement between this theory and experiment. We present a detailed account of the method, a complete set of tight-binding parameters, and results for twenty-nine of the alkaline earth, transition and noble metals.

I. INTRODUCTION

Recently, a total energy tight-binding (TB) method was introduced[1] wherein the parameters were fit to the total energies and band structures obtained from a limited set of first-principles calculations. The method produces very good structural energy differences, elastic constants, phonon frequencies, vacancy formation energies, and surface energies for the transition and noble metals. In this paper we thoroughly examine the method for these elements, and for the alkaline earth metals.

Section II describes the method, including the analytic expressions for the tight-binding parameters and the scheme for fitting them to first-principles theory. The remainder of the paper discusses the predictions made by this method. Sec. III shows that the method correctly predicts the ordering of several metallic phases, including the 29 atom αMn phase, and correctly predicts the energy differences between the lower phases. Sec. IV discusses the calculation of elastic constants. Since these calculations can also be performed by first-principles techniques,[2-5] we compare our TB results to those obtained from first-principles to assess the accuracy of the method. We can also use the method to study systems which have relatively large (20-200 atom) unit cells, a regime which requires laborious first-principles calculations, but which can be done very quickly by our TB method. In Sec. V we discuss the structure and energetics of vacancies, and in Sec. VI we consider surface energetics. Finally, in Sec. VII we summarize our results, discuss possible methods to improve our agreement with first-principles theory or experiment, and consider the course of future improvements to the method.

II. THE TIGHT-BINDING METHOD

Density functional theory (DFT),[6] using the Kohn-Sham *ansatz* for the kinetic energy,[7] tells us that the total energy of a system of electrons moving in a solid can be written in the form

$$E[n(\mathbf{r})] = \sum_i f(\mu - \varepsilon_i)\varepsilon_i + F[n(\mathbf{r})] , \qquad (1)$$

where $n(\mathbf{r})$ is the electronic density, ε_i is the Kohn-Sham eigenvalue of the ith electronic state, μ is the chemical potential, and the sum is over all electronic states of the system. Since we will be primarily interested in studying metals, we take the function $f(\mu - \varepsilon)$ to have the Fermi function form:[8]

$$f(z) = \frac{1}{1 + e^{\beta z}} , \qquad (2)$$

where $\beta = 1/(kT)$. Typically we take T between 2 and 5 mRy. The functional $F[n(\mathbf{r})]$ contains the remaining part of the DFT total energy: the ion-ion interaction energy, the parts of the Hartree and Exchange-Correlation energy not included in the eigenvalue sums, and corrections for double counting in the eigenvalue sums.

Many tight-binding methods use (1) to provide a natural separation between the parts of $E[n(\mathbf{r})]$ which can be treated by tight-binding and the parts which must be treated by other means.[9-16] In these cases the eigenvalue sum is calculated by tight-binding methods, and $F[n(\mathbf{r})]$ is approximated by a sum of pair potentials.

We have developed an alternative method of applying tight-binding to (1),[1] based on the fact that the Kohn-Sham method allows an arbitrary shift in the potential. If this shift is defined to be

$$V_0 = F[n(\mathbf{r})]/N_e , \qquad (3)$$

where

$$N_e = \sum_i f(\mu - \varepsilon_i) \qquad (4)$$

is the number of electrons in the system, then the eigenvalues ε_i are each shifted by an amount V_0, to the new values

$$\varepsilon_i' = \varepsilon_i + V_0 \ . \qquad (5)$$

The total energy (1) then becomes

$$E[n(\mathbf{r})] = \sum_i f(\mu' - \varepsilon_i')\varepsilon_i' \ , \qquad (6)$$

where $\mu' = \mu + V_0$ is the shifted chemical potential.

By the density functional theorem,[6] the shifted eigenvalues ε_i' can be considered to be functions of the crystal structure, including volume, primitive lattice vectors, and internal parameters. A tight-binding method which reproduces the ε_i' over a range of structures will then solve the total energy problem (1) or (6) without resort to an additional term.

The two-center Slater-Koster formulation[17] of tight-binding with a non-orthogonal basis breaks the problem into the calculation of three types of parameters: on-site parameters, which represent the energy required to place an electron in a specific orbital, Hamiltonian parameters, which represent the matrix elements for electrons hopping from one site to another, and overlap parameters, which describe the mixing between the non-orthogonal orbitals on neighbor sites. The eigenvalues ε_i' can be determined once the parameters are evaluated for a given structure. The basic method we use is to give the Slater-Koster parameters simple algebraic forms, with parameters chosen to reproduce first-principles results over a wide range of structures.

In an orthogonal tight-binding calculation, applying the shift (5) to each eigenvalue would be equivalent to shifting each diagonal element of the Hamiltonian matrix by an amount V_0. In the non-orthogonal case the effect is slightly more complicated. It is clear, however, that the Hamiltonian and overlap parameters should not directly depend on the shift V_0. Thus the effect of (5) can only be accounted for by changing the on-site parameters. These parameters must now be sensitive to the local environment around each atom. We describe this local environment by introducing a "density" associated with each atom, defined by

$$\rho_i = \sum_{j \neq i} \exp[-\lambda_{\tilde{j}\tilde{i}}^2 R_{ij}] F_c(R_{ij}) \ , \qquad (7)$$

where $\tilde{i}$ ($\tilde{j}$) denotes the type of atom on site i (j), λ is a parameter which will depend on the atom types, R_{ij} is the distance between atoms i and j, and $F_c(R)$ is a smooth cutoff function,

$$F_c(R) = \{1 + \exp[(R - R_0)/\ell]\}^{-1} \ , \qquad (8)$$

which we use to limit the range of the parameters. In the calculations shown here we typically take $R_0 = 14.0$ Bohr and $\ell = 0.5$ Bohr, which effectively zeros all interactions for neighbors more than 16.5 Bohr apart. Depending on the structure and lattice constant, this radius will include from 80 to 300 neighboring atoms.

Although in principle the on-site terms should have off-diagonal elements due to the overlap of the on-site wave functions with neighboring atomic potentials,[18] we follow traditional practice and only include the diagonal terms, keeping only the terms corresponding to s, p, and d orbitals. The on-site term for atom i is

$$h_{i\alpha} = a_{\tilde{i}\alpha} + b_{\tilde{i}\alpha}\rho_i^{2/3} + c_{\tilde{i}\alpha}\rho_i^{4/3} + d_{\tilde{i}\alpha}\rho^2 \ , \qquad (9)$$

where $\alpha = s, p$, or d, and ρ_i is given by (7). To show the correspondence between this theory and previous theories, note that ρ in (7) has a form similar to a pair potential. Thus if (9) were linear in ρ, we restricted ourselves to an orthogonal Hamiltonian, and kept $h_{i\alpha}$ independent of the angular momentum, then (9) would just be a method of parametrizing $F[n(\mathbf{r})]$ by a simple pair potential. Seen in this light, the density dependent parts of on-site term (9) can be regarded as a generalized pair potential.

In general the Hamiltonian and overlap Slater-Koster parameters may depend upon the structure and local environment of the atoms, even in the case of the two-center approximation. This approach, while valid, will lead to many complications when we extend the method to include other crystal structures and binary alloys. We therefore constrain the form of these parameters so that they depend only on the distance between the two atoms. Both the Hamiltonian and overlap parameters are assumed to have the same functional form,

$$P_\gamma(R) = (e_\gamma + f_\gamma R) \exp[-g_\gamma^2 R] F_c(R) \ , \qquad (10)$$

where γ indicates the type of interaction (e.g. $ss\sigma$, $pd\pi$, etc.), R is the distance between the atoms, and $F_c(R)$ is given by (8).
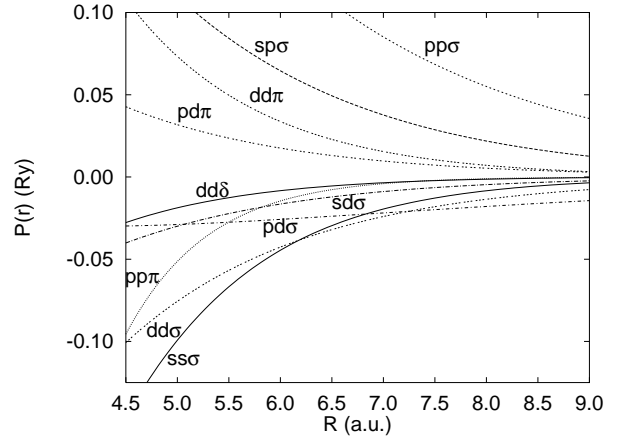
FIG. 1. Values of the two center Slater-Koster integrals for the Hamiltonian matrix as a function of distance for molybdenum, obtained from the tight-binding parameters (10). The integrals are labeled according to the standard notation.[17,19]

In the monatomic case, restricting ourselves to s, p, and d orbitals, there are three on-site Slater-Koster parameters (9), with thirteen parameters required to completely specify them. Similarly, there are ten Hamiltonian and ten overlap parameters (10), each requiring three parameters. Thus to completely specify the

Mo BCC SK

FIG. 2. The tight-binding electronic band structure of bcc Mo at the LDA equilibrium lattice constant (3.12Å). The energies of the eigenstates have been uniformly shifted to set the Fermi level to zero.

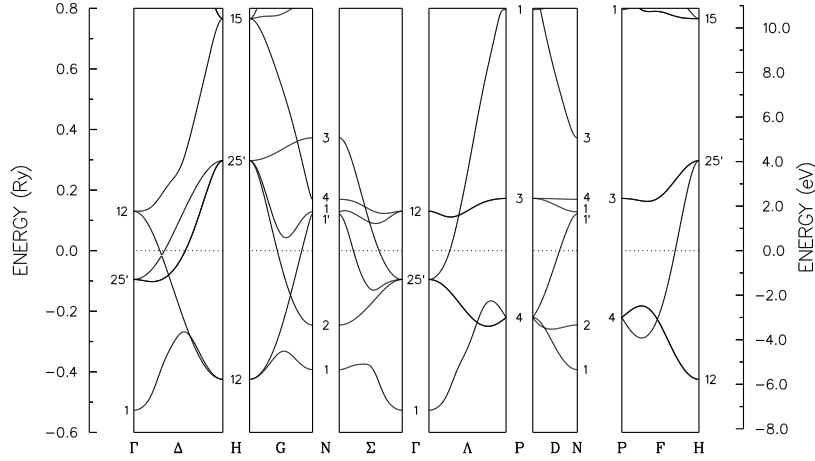Slater-Koster tight-binding scheme in this model requires the determination of at most seventy-three parameters. In practice, we only used the $d_{\tilde{i}\alpha}$ found in (9) in the parametrization of Ti, Zr, and Hf, so for most elements we had only seventy independent parameters. The parameters are determined by requiring that the eigenvalues determined by the Slater-Koster parameters[19] (7-10) reproduce the electronic band structure (including the eigenvalue shift (3)) produced by a set of first-principles density functional calculations, and that the corresponding energies (6) reproduce the first-principles energies. For the metals discussed here we use either the muffin-tin potential Augmented Plane Wave (APW)[20] or the full-potential Linearized Augmented Plane Wave (LAPW)[21,22] method to calculate the electronic band structure and total energies for 4-6 volumes in each of the fcc and bcc structures, using uniform k-point meshes which include the origin and contain 89 and 55 points, respectively. In all cases we used the Hedin-Lundqvist parametrization[23] of the Local Density Approximation[7] (LDA) to DFT. Possible spin polarization is ignored. For a typical transition metal there are about 4000 eigenvalues and energies in the database. We use an IMSL package, based on a finite difference Levenberg-Marquardt algorithm,[24] to adjust the seventy (or seventy-three) parameters to reproduce this database by means of a non-linear least squares fit, with the total energies typically weighted about 200 times larger than the eigenvalues in a single band. We place additional conditions on the minimization as follows: Since the overlap matrix defined by the parameters (10) must, physically, be positive definite, a function which penalizes small or negative determinant overlap matrices is included. While this does not guarantee that our overlap matrix will remain positive definite during the minimization process, it does tend to keep the

determinant from changing sign, meaning that an overlap matrix which is originally positive definite tends to stay that way. We also restrict the behavior of the functions (10). Physically, we expect both the Hamiltonian and Overlap parameters to decay steadily and not change sign for distances R near or greater than the nearest neighbor distance. We thus add another contribution to our minimization function, which penalizes parameter sets (e_γ, f_γ, g_γ) which cause the either $P_\gamma(r)$ or $P'_\gamma(r)$ to vanish over the range of distances where we are likely to require evaluation of the Slater-Koster matrix elements. Finally, we select our starting parameters guided by those found in previous work,[19] and ensure that the symmetry of the eigenstates is taken into account.

As an illustration of the above technique, we present several results for molybdenum. Using the APW program, we calculated the total energy and band structure of Mo at four volumes in the fcc structure and five volumes in the bcc structure. The parameters in (7), (9), and (10) were then adjusted to best fit the total energies and the band structure in the lower six bands of Mo over all nine volumes. The resulting two center Slater-Koster parameters (10) are shown in Figure 1 for the Hamiltonian matrix elements. We note that there is a smooth and monotonic decay of the TB parameters towards zero. To assess the quality of the fit, we calculate the tight-binding band structure of Mo at the LDA equilibrium volume (3.12Å) of the bcc structure (Figure 2) and compare it to the first-principles band-structure (Figure 3).[19] We see that the band structures are in close agreement over the entire Brillouin zone and a wide spectrum of energies, with some deterioration far above the Fermi level. We also calculate the energy/volume behavior for a large number of phases, and compare the fcc and bcc energies to those obtained from APW calculations, as shown
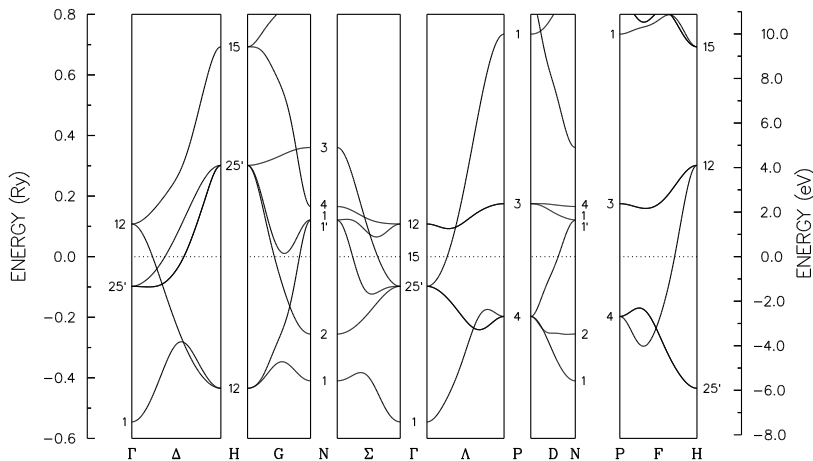
3

Mo BCC APW

FIG. 3. The self-consistent first-principles LDA electronic band structure of bcc Mo at the LDA equilibrium lattice constant (3.12Å), as determined by the muffin-tin APW program.[20] The energies of the eigenstates have been uniformly shifted to set the Fermi level to zero.

in Figure 4. We see that there is excellent agreement between the tight-binding and first-principles curves for the fcc and bcc structures, and that all other structures, including hcp, are above the bcc ground state.
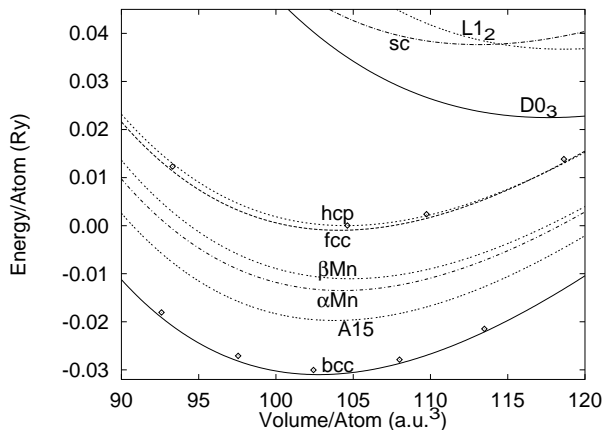

FIG. 4. The energy/volume behavior of molybdenum in several phases, using the tight-binding method. The energy of the diamond structure is not shown, as its minimum energy is 0.116 Ry above the origin. The small symbols ($\diamond$) represent the APW energies of the bcc and fcc phases. The construction of the $L1_2$ and $D0_3$ lattices is discussed in Table II. The origin of the energy was chosen arbitrarily.

The above procedure works well for all of the metals described here except vanadium, where the elastic constant C_{44} is predicted to be 172 GPa, compared to 30 GPa found experimentally[25] and 43 GPa when found using the first-principles LAPW method. This discrepancy is probably due to the high electronic density of states in vanadium near the Fermi level.[19] To better describe the electronic structure of vanadium we have made two changes to the above formalism. First, we split the d on-site energy (9) into contributions from the $t2g$ and eg levels.[19] Second, we increase our parameter space by modifying the Slater-Koster parameter's functional form (10) to include a quadratic term,

$$P_\gamma(R) = (e_\gamma + f_\gamma R + \overline{f}_\gamma R^2) \exp[-g_\gamma^2 R] F_c(R) \ . \quad (11)$$

This procedure adds an additional twenty-four parameters to our basis set, for a total of ninety-seven. We reduce this by setting $d_\alpha = 0$ in (9) for $\alpha = s$, p, $t2g$, and eg. When we fit the remaining ninety-three parameters, as above, we reduce the predicted elastic constant C_{44} to 92 GPa without significantly changing our other predictions. While this is not in perfect agreement with experiment, it is a substantial improvement, so we will use these parameters for vanadium in preference to the seventy-three parameter set which gives a worse elastic constant.

We have used this method to determine tight-binding parameters for most of the alkaline earth, transition and noble metals. In the case of the anti-ferromagnetic (Cr and Mn) and magnetic (Fe, Co, and Ni) elements we restricted our calculations to the non-magnetic case. This causes some difficulty when comparing our results to experiment, as shown below. The parameters for La are not presented because its f bands are located in the middle of the d bands[19] and therefore it is impossible to fit within our formalism. The Appendix lists various methods of obtaining the parameters used in this paper.

4

TABLE I. Equilibrium lattice constants and bulk moduli for the experimentally observed ground state structures of the elements, comparing the results of our tight-binding parametrization (TB), first-principles full potential LAPW results (LAPW), where available, and experiment (Exp.).[27,28] Where not referenced, the LAPW results were done for this paper, using previously developed methods.[4]

| Element | Structure | a (Å) | | | c (Å) | | | B_0 (GPa) | | |
		TB	LAPW	Exp.	TB	LAPW	Exp.	TB	LAPW	Exp.
Ca	fcc	5.30	5.34[a]	5.58	a	a	a	21	19[a]	15
Sc	hcp	3.26		3.31	4.91		5.27	63		44
Ti	hcp	2.97	2.87	2.95	4.80	4.55	4.68	122	120	105
V	bcc	2.94	2.93	3.03	a	a	a	211	196	162
Cr	bcc	2.80[b]		2.88	a		a	283		190
Mn	αMn	8.41[b]		8.91	a		a	320		60
Fe	bcc	2.71[b]		2.87	a		a	281		168
Co	hcp	2.40[b]		2.51	3.90[b]		4.07	384		191
Ni	fcc	3.43[b]	3.42[c]	3.52	a	a	a	268	261	186
Cu	fcc	3.52	3.52	3.61	a	a	a	189	190	137
Sr	fcc	5.73		6.08	a	a	a	15		12
Y	hcp	3.59		3.65	5.35		5.73	46		37
Zr	hcp	2.99		3.23	5.57		5.15	108		83
Nb	bcc	3.25	3.25	3.30	a	a	a	187	193	170
Mo	bcc	3.12	3.12[c]	3.15	a	a	a	283	291[c]	272
Tc	hcp	2.72		2.74	4.34		4.40	304		297
Ru	hcp	2.68		2.71	4.26		4.28	360		321
Rh	fcc	3.77	3.76	3.80	a	a	a	306	309	270
Pd	fcc	3.85	3.85	3.89	a	a	a	212	220	181
Ag	fcc	4.01	4.01	4.09	a	a	a	142	142	101
Ba	bcc	4.82		5.02	a	a	a	10		10
Hf	hcp	3.07		3.19	5.08		5.05	111		109
Ta	bcc	3.30	3.24	3.30	a	a	a	185	224	200
W	bcc	3.14	3.14	3.16	a	a	a	319	333	323
Re	hcp	2.78		2.76	4.39		4.46	371		372
Os	hcp	2.75		2.74	4.31		4.32	441		418
Ir	fcc	3.86	3.82[c]	3.84	a	a	a	389	401[c]	355
Pt	fcc	3.90	3.90	3.92	a	a	a	318	305	278
Au	fcc	4.06	4.06	4.08	a	a	a	187	205	173

[a]First-principles LAPW calculations.[3]

[b]Non-magnetic calculation. The experimental structure exhibits some form of magnetism.

[c]First-principles LAPW calculations.[5]

III. GROUND STATE BEHAVIOR AND PHASE STABILITY

We first test our parameter sets by looking at the equation of state for the observed ground state of each element. For the fcc and bcc non-magnetic cubic crystals, our parameters should reproduce the first-principles results for these phases because of the fitting procedure. For the hcp elements and manganese, these calculations serve as a tight-binding prediction of the equation of state. The case of manganese has been discussed in more detail elsewhere.[26]

Table I shows the equilibrium lattice constants and bulk moduli for all of the metals studied here, comparing them to first-principles LAPW calculations[3,5] and to experiment.[27,28] For the non-magnetic cubic crystals, the equilibrium lattice constant is within 1% of the first-principles LDA value for all of the cubic elements except

tantalum and iridium, and in these cases the discrepancy is less than 2%. Similarly, the equilibrium bulk moduli are in good agreement with the first-principles results, within 10% for all non-magnetic cubic elements except tantalum, where the error is 17%.

The hexagonal close packed phases were not fit to first-principles results. As a result, the equations of state predicted by the tight-binding model are not as accurate as for the cubic lattices. The largest error is for zirconium, where a is 7% smaller than experiment and c is 8% larger. Yttrium and hafnium also show large discrepancies between the tight-binding model and experiment, and the c for titanium is 2.5% larger than experiment. The lattice constants for the other elements are within 2% of experiment, consistent with the errors we would find in first-principles calculations. We conclude that the tight-binding method is nearly as good as first-principles LDA methods in determining the structural parameters of hcp

TABLE II. Relative energies per atom of several structures for each of the metals examined by the tight-binding model discussed in the text. The energy of the experimental ground state structure is arbitrarily set to zero. All energies are calculated at the equilibrium volume found by the tight-binding fit, and are expressed in mRy. Below the common name of each phase is its *Strukturbericht* designation.

| Element | Structure | | | | | | | | | |
| | fcc | bcc | hcp | diamond | sc | αMn | βMn | βW | AuCu$_3$ | AlFe$_3$ |
	A1	A2	A3	A4	A$_h$	A12	A13	A15	L1$_2$[a]	D0$_3$[b]
Ca	0.0	2.8	0.5	83.5	13.3	2.1	3.1	0.7	19.8	24.4
Sc	4.7	8.5	0.0	101.1	34.3	10.2	11.0	19.4	39.7	33.9
Ti	5.2	9.1	0.0	157.7	64.9	16.7	15.4	22.4	56.1	63.8
V	19.6	0.0	19.6	180.8	76.0	11.2	12.7	12.2	62.1	53.4
Cr	28.6	0.0	30.6	49.1	118.6	20.3	19.7	16.2	94.3	87.2
Mn	7.5	14.3	2.9	44.2	90.3	0.0	1.5	7.0	87.6	66.2
Fe	-27.9	0.0	-35.0	79.8	54.5	-23.1	-25.0	-8.1	4.5	20.4
Co	-2.9	21.0	0.0	135.0	8.2			19.2	72.7	75.2
Ni	0.0	8.0	2.8	142.3	75.9	7.7	4.6	15.0	48.7	57.1
Cu	0.0	3.5	1.2	70.8	24.7	6.2	5.4	10.1	14.7	22.0
Sr	0.0	2.1	1.0	73.0	22.0	3.2	3.2	1.4	22.2	25.4
Y	2.4	8.8	0.0	97.9	432.2	8.6	10.4	17.3	31.5	27.5
Zr	1.1	2.9	0.0	112.7	123.3	8.6	8.0	8.0	18.7	26.2
Nb	26.1	0.0	22.7	181.9	68.6	17.1	21.1	15.9	69.5	59.6
Mo	30.0	0.0	31.0	147.3	68.7	17.5	19.9	11.3	67.7	53.5
Tc	6.1	23.3	0.0	72.9	56.3	0.2	4.5	13.3	64.6	35.4
Ru	1.0	44.6	0.0	134.5	106.6	16.3	14.6	34.7	103.0	82.7
Rh	0.0	31.7	5.1	159.8	96.0	16.3	7.4	29.5	81.2	88.3
Pd	0.0	9.9	2.5	148.6	84.9	9.2	6.1	12.8	50.1	72.8
Ag	0.0	3.3	0.6	66.1	24.1	6.0	5.3	8.6	15.7	25.2
Ba	0.9	0.0	0.1	85.3	23.6	2.8	2.9	2.2	27.0	30.7
Hf	1.2	7.1	0.0	380.2	113	22.9	20.6	20.8	110.2	143.3
Ta	24.7	0.0	25.3	188.6	63.2	8.9	14.0	9.8	65.6	54.2
W	36.0	0.0	10.1	159.3	113.7	18.2	25.7	12.4	134.2	94.2
Re	13.4	27.7	0.0	28.6	55.6	0.2	1.8	19.1	61.0	22.1
Os	8.1	64.3	0.0	11.2	58.6	17.8	17.4	42.4	66.2	33.6
Ir	0.0	50.1	8.5	83.9	83.5	23.8	19.9	41.8	64.0	75.6
Pt	0.0	9.7	4.4	168.7	78.3	14.4	12.8	25.9	48.5	78.5
Au	0.0	1.4	0.6	96.1	24.1	8.7	8.4	15.2	17.5	32.3

[a]Calculations using the L1$_2$ (AuCu$_3$) lattice, placing the metal atoms on the copper sites and leaving vacancies on the gold sites.

[b]Calculations using the D0$_3$ (AlFe$_3$) lattice, placing the metal atoms on the iron sites and leaving vacancies on the aluminum sites.

metals.

To be successful, the tight-binding method must also show that the experimental ground state structure is, in fact, the ground state predicted by the method. We have calculated energy versus volume curves for several common crystal structures. As an example, Figure 4 shows the resulting energy/volume curves for molybdenum. The results for all of the elements are summarized in Table II, which shows the equilibrium energy of each of these phases expressed as the difference in energy between that phase and the equilibrium energy of the experimental ground state. The c/a ratio of the hcp phase has been chosen to minimize the tight-binding energy at each volume to obtain the hcp energies. The tight-binding method correctly predicts the ground state structure for all metals except the ferromagnetic metals iron and cobalt. This is understandable, since we have not included spin-polarization. Especially satisfying is the fact the method finds the correct ground states of the hcp metals and manganese,[26] since these phases are not included in the fit of the tight-binding parameters.

We can also assess the stability of the tight-binding parameters by studying crystal structures of lower symmetry. Thus Figure 5 shows the energy of molybdenum under a volume conserving tetragonal strain, the so-called Bain path,[29] at the experimentally observed equilibrium volume of the bcc phase. The energy is properly a minimum for the bcc lattice, where $c/a = 1$, and attains a local maximum at the fcc structure ($c/a = \sqrt{2}$), indicating that $C_{11} - C_{12} < 0$, so that the fcc structure is unstable. Similarly, Figure 6 shows the energy for a monatomic lattice undergoing a trigonal strain with the primitive vectors
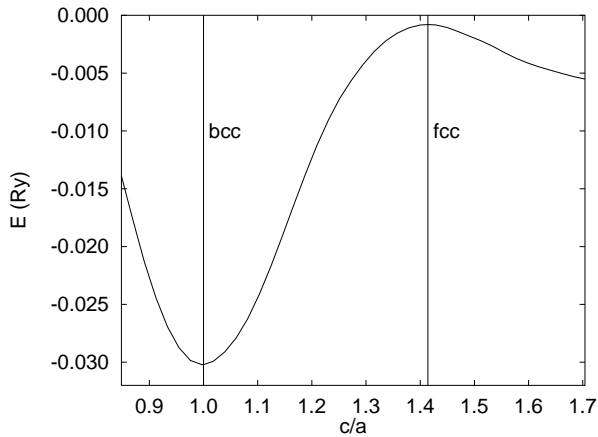
FIG. 5. The tight-binding calculation of the energy of molybdenum, at the experimental equilibrium volume, under a tetragonal strain (the Bain path[29]), as a function of c/a. The vertical lines denote the positions of the bcc and fcc lattices.

$$\begin{pmatrix} \mathbf{a}_1 \\ \mathbf{a}_2 \\ \mathbf{a}_3 \end{pmatrix} = \begin{pmatrix} \alpha & \beta & \beta \\ \beta & \alpha & \beta \\ \beta & \beta & \alpha \end{pmatrix} \begin{pmatrix} \hat{x} \\ \hat{y} \\ \hat{z} \end{pmatrix} , \qquad (12)$$

where α and β are chosen so that the volume is the experimentally observed volume of the bcc lattice, and the angle between the primitive vectors is given by θ, where

$$\cos\theta = \frac{(2\alpha + \beta)\beta}{\alpha^2 + 2\beta^2} . \qquad (13)$$

The vectors (12) represent an fcc lattice when $\theta = 60 \deg$, a simple cubic lattice when $\theta = 90 \deg$, and a bcc lattice when $\theta = 109.47 \deg$. The tight-binding calculations in Figure 6 show that the bcc phase is, indeed, the minimum energy structure. Also, the simple cubic phase has a local maximum in the energy, indicating that it is elastically unstable with $C_{44} < 0$.

IV. ELASTIC CONSTANTS

Elastic constants are calculated by imposing an external strain on the crystal, relaxing any internal parameters to obtain the energy as a function of the strain, and numerically solving for the elastic constants as the curvature of the energy versus strain curve.[2–5] We have calculated the elastic constants for the ground state phases of all of the elements in this study except manganese. This procedure serves two purposes: it tests the mechanical stability of the tight-binding ground state; and it assesses the ability of the method to determine properties not included in the fit of the tight-binding parameters.

The elastic constants of the cubic materials (except manganese) are shown in Table III. This table also shows the elastic constants obtained from first-principles LAPW computations[5] and experiment.[25,30,31] All calculations were performed at the experimental volume. The
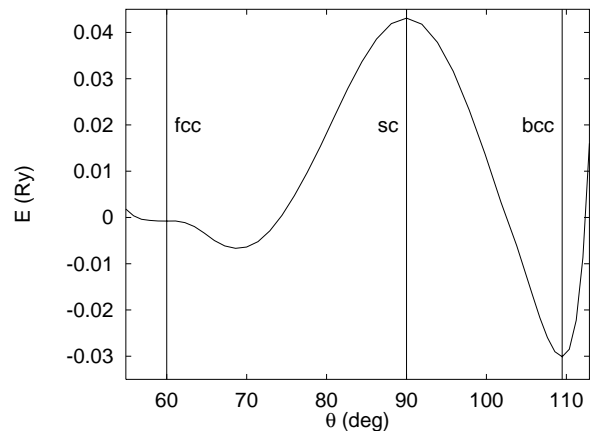
FIG. 6. The tight-binding calculation of the energy of molybdenum, at the experimental equilibrium volume, under a trigonal strain of the lattice given by (12), as a function of the angle between the primitive vectors, θ. The positions of the bcc, simple cubic, and fcc lattices are denoted by the vertical lines.

accuracy of the elastic constants C_{11} and C_{12} is remarkably good. For the twelve elements for which we have first-principles results, none of the tight-binding elastic constants differs from the first-principles results by more than 15%. For comparison, the first-principles results also differ from the experimental results by less than 15%, a measure of the accuracy of the LDA in determining these elastic constants. Thus the tight-binding elastic constants are not significantly worse than those computed from first-principles. Considering only the non-magnetic materials, the root-mean-square (RMS) deviation of the tight-binding C_{11} compared to experiment is 38 GPa, while the RMS deviation of C_{12} is 15 GPa.

The errors in C_{44} are somewhat larger, the RMS deviation from experiment being 49 GPa. In this case, if we exclude calcium and strontium, discussed below, the maximum deviation of first-principles results from experiment is 22%, in molybdenum. The maximum deviation of the tight-binding elastic constant from the first-principles result is in vanadium, where the error is 114%, even when we use the quadratic Slater-Koster parametrization (11) and split the on-site d terms. As noted above, this is probably due to the high value of the density of states of vanadium near the Fermi level.[19] Excluding vanadium, the maximum deviation is 36%, in niobium. For comparison, the first-principles results differ from experiment by at most 22%, in molybdenum. Hence, except for the anomaly of vanadium, the tight binding results are only slightly worse than the first-principles results in the determination of elastic constants.

Calculation of C_{44} in the alkaline earth metals is difficult because the lattice is extremely soft. The error in calcium is 71%, compared to first-principles results, and 50% compared to experiment. For strontium the situation is even worse, since we predict the fcc lattice to be unstable to any strain which is related to C_{44}. In this

TABLE III. Elastic constants for cubic elements. All elements for which we have constructed a set of tight-binding parameters and which have a cubic ground state (except manganese) are presented here. Comparison is made between the results of our tight-binding parametrization (TB), first-principles full potential LAPW results (LAPW), where available, and experiment (Exp.).[25] Where unreferenced, the LAPW results were done for this paper, using previously developed methods.[4] Calculations were performed at the experimental volume.

| | C_{11} | | | C_{12} | | | C_{44} | | |
	TB	LAPW	Exp	TB	LAPW	Exp	TB	LAPW	Exp
Ca	15	17[a]	16[b]	10	10[a]	12[b]	4	14[a]	8[b]
V	224	205	228	106	111	119	92	30	43
Cr	432		346	88		66	250		100
Fe	-4			227			180		
Ni	256			142			86		
Cu	161	156	168	108	106	121	55	80	75
Sr	8		15	3		6	-3		10
Nb	204	230	246	137	122	139	34	25	29
Mo	453	468[a]	450[c]	147	149[a]	173[c]	120	98[a]	125[c]
Rh	491	433	413	171	185	194	260	206	184
Pd	233	218	227	163	172	176	63	74	72
Ag	133	122	124	86	90	93	42	52	46
Ba	9			7			13		
Ta	275	256	261	140	154	157	78	67	82
W	529	527	523	170	194	203	198	147	160
Ir	694	621[a]	590	260	256[a]	249	348	260[a]	262
Pt	380	381	347	257	189	251	71	83	76
Au	184	200	189	154	173	159	43	33	42

[a]First-principles LAPW calculations.[5]
[b]Experiment[30]
[c]Experiment[31]

regard, however, it is important to note that even many of the best LDA elastic constant calculations in Table III have an absolute error of more than 10 GPa. Since the experimental values of C_{44} for both calcium and strontium are less than 10 GPa, it is understandable that we cannot reproduce the experimental elastic constants for the alkaline earth metals with any degree of accuracy.

We also note that this method correctly reproduces the sign of the elastic constant $C_{12} - C_{44}$, even in rhodium and iridium, where it is negative, though the predicted magnitude $|C_{12} - C_{44}|$ is much larger than observed experimentally and in first-principles calculations for these two materials. The negative sign cannot be obtained from the standard Embedded Atom Method (EAM),[32] though it can be found in the Modified Embedded Atom Method (MEAM).[33]

We have also calculated elastic constants for all of the non-magnetic transition metals which take the hcp structure. Hexagonal close packed crystals have two atoms per unit cell, and the internal parameter describing the atomic positions is free to move when we strain the crystal to calculate elastic constants. Using the tight-binding approach, it is relatively simple to determine the value

TABLE IV. Elastic constants for hexagonal close-packed elements. All elements for which we have constructed a set of tight-binding parameters and which have a non-magnetic *hcp* ground state are presented here. Comparison is made between the results of our tight-binding parametrization (TB) and experiment (Exp).[30] The tight-binding results include internal relaxation. Calculations were performed at the experimental volume, but at the c/a ratio which minimized the energy for that volume. Note that in a hexagonal crystal, $C_{66} = (C_{11} - C_{12})/2$.

| | C_{11} | | C_{12} | | C_{13} | | C_{33} | | C_{44} | |
	TB	Exp	TB	Exp	TB	Exp	TB	Exp	TB	Exp
Sc	73	99	30	40	31	29	78	107	25	28
Ti	171	160	58	90	46	60	203	181	64	47
Y	45	78	15	29	13	20	48	77	17	24
Zr	102	144	67	74	65	67	99	166	4	33
Tc	477		196		172		505		127	
Ru	642	563	170	188	129	168	706	624	214	181
Re	559	616	283	273	250	206	621	683	136	161
Os	754		272		274		831		232	

of the internal parameter which minimizes the total energy for a given external strain, and then find the related elastic constant by standard techniques. This is more difficult for first principles calculations, so we have not calculated LAPW elastic constants for hexagonal materials. The tight-binding elastic constants are compared to experiment[30] in Table IV. For simplicity in interpreting the results, we calculated the elastic constants using the tight-binding c/a ratio at the experimental volume. The hcp tight-binding elastic constants show larger relative deviations from experiment than found in the cubic crystals. The largest deviation, 88%, occurs in the calculation of C_{44} in zirconium, where we predict a value of 4 GPa, compared to the 33 GPa found by experiment. The RMS deviations of the tight-binding elastic constants from experiment are 46 GPa for C_{11}, 17 GPa for C_{12}, 25 GPa for C_{13}, 54 GPa for C_{33}, and 22 GPa for C_{44}. The RMS deviation over all of the hcp elastic constants is 36 GPa. When compared to the RMS deviation for cubic materials (37 GPa), we see that on average the hcp elastic constants are as accurate as those calculated in the cubic case.

V. VACANCIES

Vacancy formation energies are most easily determined by the supercell total-energy method.[34] One atom in the supercell is removed, and neighboring atoms are allowed to relax around this vacancy while preserving the symmetry of the lattice. The great advantage of the tight-binding method over first-principles calculations is that we can do the calculation in a very large supercell, eliminating the possibility of vacancy-vacancy interactions. We find that a supercell containing 108 atoms is suffi-

TABLE V. Tight-binding vacancy formation energies compared to first-principles calculations and experiment. Energies were computed using a 108 atom supercell. Calculations with the atoms at the primitive lattice sites in the crystal (Fixed) and allowing relaxation around the vacancy (Relaxed) are shown. First-principles calculations of the vacancy formation energy are given in the column labeled "LDA". The experimental column shows a range of energies if several experiments have been tabulated. Otherwise the estimated error in the experiment is given.

Element	Vacancy Formation Energy			
	Tight-Binding		LDA	Experiment[a]
	Fixed	Relaxed		
Cu	1.29	1.18	1.41[b] 1.29[c]	1.28 - 1.42
Nb	2.84	2.82		2.65 ± 0.3
Mo	2.63	2.46		3.0 - 3.6
Rh	3.39	3.35	2.26[c]	1.71[d]
Pd	2.46	2.45	1.57[b]	1.85 ± 0.25
Ag	1.31	1.24	1.20[b] 1.06[c]	1.11 - 1.31
Ta	3.17	2.95		2.9 ± 0.4
W	6.86	6.43		4.6 ± 0.8
Ir	2.19	2.17		1.97[d]
Pt	2.79	2.79		1.35 ± 0.09
Au	1.24	1.12		0.89 ± 0.04

[a]Experimental energies as tabulated by Schaefer[37] unless otherwise noted.
[b]First-principles calculations of Dederichs et al..[35]
[c]First-principles calculations of Polatoglou et al.[36]
[d]Experimental energy tabulated by de Boer et al.[38]

cient to eliminate the interaction. The vacancy formation energy is given by

$$E_{vac}(V) = E_{sc}(N-1, 1; V) - (N-1)E_{bulk}(V/N) ,$$
(14)

where $E_{sc}(M, Q; V)$ is the total energy of a supercell of volume V containing M atoms and Q vacancies, and $E_{bulk}(V)$ is the energy per atom of the bulk metal at a volume V per atom. We use the experimental lattice constant to set the volume of the system, since under experimental conditions the lattice constant of a metal containing isolated vacancies will be the lattice constant of the bulk metal.

We have computed the vacancy formation energy of several of the cubic transition and noble metals using this tight binding method, including relaxation around the vacancy. The results are presented in Table V, where we also compare to first principles results[35,36] and experiment.[37,38] The calculated vacancy formation energies of niobium, silver, tantalum, and iridium are in excellent agreement with experiment. The tight-binding parametrizations of rhodium, tungsten, and platinum give the poorest vacancy formation energies, 1–2 eV above the experimental value.

We note that the $L1_2$ and $D0_3$ lattices described in Table II can be considered vacancy-containing supercells

with $N = 4$. Though the vacancy-vacancy interaction in these cells is quite large, fitting the TB parameters (7-10) to first-principles results for these lattices will improve the vacancy formation energy calculation. We have yet to implement this procedure.

VI. SURFACES

The tight-binding model can be used to calculate surface energies by the supercell technique. A slab of metal is formed by cleaving the crystal along the desired plane, creating two identical free surfaces. The distance between the two surfaces in increased, creating a set of slabs which repeat periodically in the direction perpendicular to the surfaces. Of course, we must take care to separate the slabs by a large region of vacuum so that the electrons on one slab cannot hop to a neighboring slab. The slabs must be thick enough so that the atoms at the center of the slab have the properties (e.g., local electronic density of states) of atoms in the bulk material, and so that the two surfaces on the same slab cannot interact with each other. For low index ((100), (110), and (111)) faces of the non-magnetic fcc and bcc metals we find that a slab containing 25 atomic layers is sufficient to meet these criteria. We also converge the calculations with respect to the k-point mesh. Depending on the surface and underlying bulk structure this takes between 19 and 91 k-points in the two dimensional Brillouin zone. We estimate numerical error in the TB surface energies to be about 0.1 J/m^2.

The surface energy, expressed as the energy required to create a unit area of new surface, is then given by the formula

$$E_{surf} = \frac{1}{2A}(E_{slab} - NE_{bulk})$$
(15)

where A is the area occupied by one unit cell on the surface of the slab, E_{slab} is the total energy of the slab, N is the number of atoms in the unit cell, and E_{bulk} is the energy of one atom in the bulk at the lattice constant of the atoms in the interior of the slab. For simplicity, the calculations were done using the bulk equilibrium lattice parameters, with no relaxation or reconstruction at the surface. Our calculations indicate that relaxation *energies* are on the order of 1-10% of the total surface energy, so neglecting relaxation will not significantly alter our conclusions. Of course, relaxation and reconstruction are necessary in order to understand surface properties. We will address these issues in a future paper.

We have calculated the formation energies for bulk terminated (i.e., unrelaxed and unreconstructed) low index ((100), (110), and (111)) surfaces of the non-magnetic fcc and bcc transition and noble metals. Table VI compares these results to experiment,[39,40] first-principles calculations,[36,41−44] and atomistic models.[33,45,46] Note that except for the (100) surface of tungsten, the experi-

TABLE VI. Surface energies, calculated from the tight-binding theory (TB), by first principles Local Density methods (LDA), by the embedded atom method (EAM), or by the modified embedded atom method (MEAM), compared to experiment. Energies are given in units of J/m^2.

Element	Orientation	TB	LDA	EAM	MEAM[a]	Experiment
	(111)	3.34			1.81	2.6[b]
V	(110)	2.13		1.68[c]	1.71	
	(100)	3.04		1.83[c]	2.49	
	(111)	1.73	1.94[d]	1.17[e]	1.41	1.77[f]
Cu	(110)	2.04		1.40[e]	1.64	
	(100)	1.93		1.28[e]	1.65	
	(111)	2.44			2.02	2.3[b]
Nb	(110)	1.54	2.36[g] 2.9[h]	1.81[c]	1.87	
	(100)	2.37	2.86[g] 3.1[h]	1.97[c]	2.02	
	(111)	2.84			1.86	2.9[b]
Mo	(110)	3.04	3.14[g]	2.13[c]	1.93	
	(100)	2.12	3.52[g]	2.28[c]	2.12	
	(111)	2.46	2.54[d] 2.53[g]		2.60	2.6[b]
Rh	(110)	2.71	2.88[g]		2.92	
	(100)	2.57	2.81[g]		2.90	
	(111)	1.57	1.64[g]	1.22[e]	1.38	2.00[b]
Pd	(110)	1.86	1.97[g] 2.5[h] 2.70[i]	1.49[e]	1.67	
	(100)	1.75	1.86[g] 2.3[h] 1.04[i]	1.37[e]	1.66	
	(111)	1.14	1.21[g] 1.21[d]	0.62[e]	1.09	1.32[f]
Ag	(110)	1.42	1.26[g] 1.4[h]	0.77[e]	1.27	
	(100)	1.29	1.21[g] 1.3[h]	0.71[e]	1.22	
	(111)	3.14			2.31	2.78[b]
Ta	(110)	2.05		1.80[c]	2.17	
	(100)	3.00		1.99[c]	3.29	
	(111)	6.75			2.25	2.99[f]
W	(110)	4.30		2.60[c]	2.23	
	(100)	6.7	5.54[j]	2.81[c]	2.65	6[k]
	(111)	2.59			2.84	3.0[b]
Ir	(110)	3.19			3.06	
	(100)	2.95			2.91	
	(111)	2.51		1.44[e]	1.66	2.49[b]
Pt	(110)	2.97		1.75[e]	2.13	
	(100)	2.83		1.65[e]	2.17	
	(111)	1.48		0.79[e]	0.89	1.54[f]
Au	(110)	1.85		0.98[e]	1.12	
	(100)	1.69		0.92[e]	1.08	

[a]Modified Embedded-Atom calculations.[33]

[b]Experimental determination of the surface energy of an "average" face using an approximate extrapolation to T = 0.[33]

[c]Embedded-Atom calculations for bcc metals.[46]

[d]Full-Potential Linearized Muffin-Tin Orbital (Full Potential-LMTO) calculation, using seven layer slabs.[36]

[e]Embedded-Atom calculations for fcc metals.[45]

[f]Experimental determination of the surface energy of an "average" face at T = 0.[39]

[g]FP-LMTO calculation, using seven layer slabs.[42]

[h]Full-Potential LAPW calculation, using nine layer slabs.[43]

[i]Local orbital pseudo-potential calculation, using a three layer slab.[41]

[j]Full-Potential Linearized Augmented Plane Wave (LAPW) calculation for the ideal surface, using a five layer slab.[44]

[k]Experimental result for the (100) surface.[40]

mental results[33,39] are for an "average" surface, and some are extrapolated to T = 0 from high temperatures.[33]

The results for the fcc metals are particularly gratifying. In all cases we find $E_{(111)} < E_{(100)} < E_{(110)}$. Thus close-packed surfaces are the most stable for the fcc metals. The TB surface energies are uniformly larger, and closer to experiment, than those obtained by the embedded atom method (EAM),[45] which is known to underestimate surface energies in fcc metals. Our surface energies are generally closer to experiment than those obtained by the Modified Embedded Atom Method (MEAM),[33] and in good agreement with first-principles calculations of the surface energy of copper(111),[36] and rhodium.[42] Our calculations are also in the range of the surface energies predicted by several first-principles calculations for palladium and silver.[41−43]

Results for bcc metals are also good. For all of the unrelaxed surfaces we find $E_{(110)} < E_{(100)} < E_{(111)}$. The energies for niobium and molybdenum are somewhat low compared to both first-principles calculations[42,43] and experiment, but the only serious discrepancy is the average surface energy of tungsten, which is smaller than our values by a factor of one-third. At the moment this is not particularly worrisome, because experimental estimates of the surface energy of tungsten range from 1.68 J/m^2 to 4.50 J/m^2.[47] The latter number is, in fact, in range of our calculation for the (110) surface. In addition, the results for the energy of the (100) surface of tungsten are in good agreement with both first-principles results[44] and experiment.[40]. In most cases the tight-binding surface energies are greater than either of the corresponding EAM or MEAM values. Where this is not the case the energy difference is slight.

VII. SUMMARY

We have extended the tight-binding method[1] to include most of the alkaline earth, transition, and noble metals. Tight-binding parameters are determined by doing a least squares fit to simultaneously reproduce the total energy and electronic structure determined by first-principles at several volumes of the fcc and bcc lattices. In all cases except the ferromagnetic metals the method correctly predicts the ground state structure, even when the ground state is hcp or αMn.

The method was tested against first-principles results and experiment by the calculation of elastic constants, vacancy formation energies, and surface energies. Elastic constants for non-magnetic cubic materials are, in general, in good agreement with both LAPW calculations and experiment, though we have some problems with C_{44} in vanadium. Since the tight-binding method does not require a specific sign for $C_{12} - C_{44}$ we get reasonable elastic constants even for rhodium and iridium. Elastic constants for the hcp phase are nearly as accurate as those calculated in the cubic phase.

Compared to experiment, the accuracy of the vacancy formation energy predictions range from good to poor, with niobium, silver, tantalum, and iridium all in excellent agreement with experiment, and rhodium, tungsten, and platinum much larger than experiment.

Surface energies for both fcc and bcc crystals are in good agreement with the available first-principles and experimental data. Energies for fcc crystals are uniformly larger than the corresponding EAM energies, in agreement with experiment.

Improvements to the tight-binding method are under investigation. In particular, we are examining other forms for the parametrization of the on-site terms (9) and the Slater-Koster terms (10). We are also investigating the effect of two-center Slater-Koster integrals on the on-site terms, as suggested by Mercer and Chou.[18] Since these terms properly account for the crystal-field splitting of the on-site terms, they may be useful in obtaining even more accurate results. Finally, we have begun the process of extending the tight-binding method to binary systems.[48]

APPENDIX: THE TIGHT-BINDING PARAMETERS

The tight-binding parameters used in this paper are available from the AIP Physics Auxiliary Publication Service, `http://www.aip.org/epaps/epaps.html`, as noted in a footnote to this paper, on the World Wide Web at `http://cst-www.nrl.navy.mil/bind`, or via email at `mehl@dave.nrl.navy.mil`.

TABLE VII. Tight-binding parameters (7-10) for Calcium, Scandium, Titanium, Vanadium, and Chromium. The equation numbers refer to the parametrization forms discussed in the text. Note that the $t2g$ and eg on-site parameters are identical for all elements except vanadium.

Parameter	Calcium	Scandium	Titanium	Vanadium	Chromium
			On-Site Parameters Eqs. (7) and (9)		
λ	1.12775E+00	1.16238E+00	1.30248E+00	1.578632+00	1.59665E+00
a_s	2.43912E−01	3.91870E−01	−1.53116E−02	1.24744E−01	3.57154E−01
b_s	−1.73150E+01	−1.29635E+01	1.82222E+01	−3.46195E+01	−8.83822E+00
c_s	5.96806E+02	4.06795E+02	2.12586E+03	6.62479E+04	3.91628E+04
d_s	0.00000E+00	0.00000E+00	3.35194E+03	0.00000E+00	0.00000E+00
a_p	1.67761E−01	1.08349E−01	3.73246E−01	5.09467E−01	6.65273E−01
b_p	1.87785E+01	1.49373E+01	2.87173E+01	1.22445E+02	9.54968E+01
c_p	−2.11382E+02	−6.25612E+00	−6.66496E+01	−5.81167E+03	4.05266E+02
d_p	0.00000E+00	0.00000E+00	−1.89929E+03	0.00000E+00	0.00000E+00
a_{t2g}	2.31793E−01	1.92461E−01	1.44001E−01	1.35087E−01	9.80248E−02
b_{t2g}	2.56001E+00	−4.09038E−02	5.62900E+00	2.82780E+01	3.16359E+01
c_{t2g}	4.43144E+00	4.49403E+01	−1.11934E+02	1.96581E+02	−1.70206E+03
d_{t2g}	0.00000E+00	0.00000E+00	4.39451E+03	0.00000E+00	0.00000E+00
a_{eg}	2.31793E−01	1.92461E−01	1.44001E−01	1.52188E−01	9.80248E−02
b_{eg}	2.56001E+00	−4.09038E−02	5.62900E+00	1.42941E+01	3.16359E+01
c_{eg}	4.43144E+00	4.49403E+01	−1.11934E+02	2.92193E+03	−1.70206E+03
d_{eg}	0.00000E+00	0.00000E+00	4.39451E+03	0.00000E+00	0.00000E+00
			Hamiltonian Parameters Eq. (10) or (11)		
$e_{ss\sigma}$	1.03105E+02	8.97124E+01	−3.04758E+01	3.36262E+00	3.16386E+00
$f_{ss\sigma}$	−1.75892E+01	−2.00737E+01	3.65365E−01	−1.14810E+00	−1.12865E+00
$\overline{f}_{ss\sigma}$	0.00000E+00	0.00000E+00	0.00000E+00	−7.17525E−03	0.00000E+00
$g_{ss\sigma}$	9.40409E−01	1.03023E+00	1.02322E+00	8.06897E−01	8.40762E−01
$e_{sp\sigma}$	−6.67410E+00	−5.39161E+00	2.52625E+00	9.10588E−01	1.42516E+00
$f_{sp\sigma}$	1.23384E+00	1.28676E+00	−6.91609E−02	−5.48139E−02	−5.72265E−02
$\overline{f}_{sp\sigma}$	0.00000E+00	0.00000E+00	0.00000E+00	2.14256E−02	0.00000E+00
$g_{sp\sigma}$	7.43630E−01	7.90720E−01	7.98877E−01	7.28117E−01	6.78224E−01
$e_{pp\sigma}$	−2.74551E−01	−1.23867E−01	1.15348E+00	−5.58852E−01	1.68736E+00
$f_{pp\sigma}$	1.31541E−01	1.08003E−01	−6.14491E−02	1.50760E−01	1.15999E−02
$\overline{f}_{pp\sigma}$	0.00000E+00	0.00000E+00	0.00000E+00	4.95827E−01	0.00000E+00
$g_{pp\sigma}$	6.19331E−01	6.19587E−01	5.59035E−01	7.59313E−01	7.60586E−01
$e_{pp\pi}$	−4.29276E+02	−2.38965E+01	−3.89463E+00	2.68584E+02	−4.81928E+01
$f_{pp\pi}$	4.41085E+01	−8.63951E+00	1.66898E+00	−5.61785E+01	1.44596E+01
$\overline{f}_{pp\pi}$	0.00000E+00	0.00000E+00	0.00000E+00	1.24700E+00	0.00000E+00
$g_{pp\pi}$	1.16964E+00	1.14561E+00	1.04814E+00	1.26040E+00	1.29469E+00
$e_{sd\sigma}$	9.68472E−01	5.15292E−01	−1.07381E+00	1.41944E−02	7.71274E−01
$f_{sd\sigma}$	−2.37815E−01	−1.44198E−01	6.14641E−02	−5.56681E−02	−1.62549E−01
$\overline{f}_{sd\sigma}$	0.00000E+00	0.00000E+00	0.00000E+00	−7.17105E−04	0.00000E+00
$g_{sd\sigma}$	7.16040E−01	7.61250E−01	7.50489E−01	6.69904E−01	7.41397E−01
$e_{pd\sigma}$	1.26136E+00	4.44491E−01	−3.22172E−01	4.32047E+00	4.28533E+00
$f_{pd\sigma}$	−2.09090E−01	−1.06993E−01	−2.21047E−03	−1.09109E+00	−1.06533E+00
$\overline{f}_{pd\sigma}$	0.00000E+00	0.00000E+00	0.00000E+00	−3.56750E−03	0.00000E+00
$g_{pd\sigma}$	6.70733E−01	6.36292E−01	6.24299E−01	8.19499E−01	8.40053E−01
$e_{pd\pi}$	5.57017E−01	5.24971E−01	3.19996E−01	−2.39826E+00	−2.29533E+00
$f_{pd\pi}$	−4.67466E−02	−2.50914E−02	−2.06480E−02	7.87639E−01	7.92622E−01
$\overline{f}_{pd\pi}$	0.00000E+00	0.00000E+00	0.00000E+00	−3.28881E−03	0.00000E+00
$g_{pd\pi}$	6.00789E−01	6.55945E−01	6.50894E−01	8.95260E−01	8.52608E−01

$e_{dd\sigma}$	4.76025E+00	9.13632E−01	−8.83254E−01	−1.38932E+00	−1.44185E+00
$f_{dd\sigma}$	−9.11415E−01	−2.84308E−01	−1.06276E−02	4.40043E−02	8.41726E−02
$\overline{f}_{dd\sigma}$	0.00000E+00	0.00000E+00	0.00000E+00	−9.20172E−03	0.00000E+00
$g_{dd\sigma}$	8.17314E−01	7.58386E−01	7.48868E−01	8.12780E−01	7.92347E−01
$e_{dd\pi}$	−8.83124E−01	8.09225E−01	2.14981E+00	2.44958E+00	3.37805E+00
$f_{dd\pi}$	5.71572E−01	3.86043E−01	4.84974E−02	1.90258E−01	3.41379E−02
$\overline{f}_{dd\pi}$	0.00000E+00	0.00000E+00	0.00000E+00	1.08500E+00	0.00000E+00
$g_{dd\pi}$	8.35313E−01	8.67158E−01	8.78521E−01	9.45587E−01	9.58150E−01
$e_{dd\delta}$	1.05244E+02	1.92969E+02	1.26999E+01	1.52551E+02	−1.14015E+01
$f_{dd\delta}$	−1.89498E+01	−3.97738E+01	−1.04051E+01	−1.85124E+02	5.73356E−01
$\overline{f}_{dd\delta}$	0.00000E+00	0.00000E+00	0.00000E+00	−1.58858E+00	0.00000E+00
$g_{dd\delta}$	1.07735E+00	1.18457E+00	1.27903E+00	1.52346E+00	1.18366E+00
Overlap Parameters Eq. (10) or (11)					
$e_{ss\sigma}$	7.92707E+00	4.81308E+00	1.13429E+00	−6.01744E−01	−1.90233E+00
$f_{ss\sigma}$	−7.22811E−01	−5.79825E−01	−1.19576E−02	9.74987E−01	1.28953E+00
$\overline{f}_{ss\sigma}$	0.00000E+00	0.00000E+00	0.00000E+00	2.92855E−03	0.00000E+00
$g_{ss\sigma}$	6.64862E−01	7.13371E−01	6.96534E−01	7.63881E−01	8.44029E−01
$e_{sp\sigma}$	5.42081E+04	2.63307E+04	−6.19606E+01	9.22403E−01	6.30159E+00
$f_{sp\sigma}$	−8.78337E+03	−5.56247E+03	5.18187E−01	−1.85853E+00	−1.59725E+00
$\overline{f}_{sp\sigma}$	0.00000E+00	0.00000E+00	0.00000E+00	−2.50567E−01	0.00000E+00
$g_{sp\sigma}$	1.22836E+00	1.35254E+00	1.13620E+00	8.16578E−01	8.56016E−01
$e_{pp\sigma}$	2.93593E+01	6.97663E+00	−3.75786E+01	1.27358E+01	8.43048E+00
$f_{pp\sigma}$	−6.62151E+00	−1.72009E+00	1.08078E+01	−3.00275E+00	−2.13782E+00
$\overline{f}_{pp\sigma}$	0.00000E+00	0.00000E+00	0.00000E+00	−2.76667E−02	0.00000E+00
$g_{pp\sigma}$	8.46628E−01	7.93212E−01	1.04440E+00	7.60395E−01	7.01353E−01
$e_{pp\pi}$	−2.47333E+02	−1.43227E+01	4.34031E+00	−2.56081E+00	−2.19353E+00
$f_{pp\pi}$	4.47028E+01	3.41589E+00	−3.75328E−03	1.61177E+00	1.07267E+00
$\overline{f}_{pp\pi}$	0.00000E+00	0.00000E+00	0.00000E+00	−1.07454E−01	0.00000E+00
$g_{pp\pi}$	9.65850E−01	8.08203E−01	8.60463E−01	7.30749E−01	7.56032E−01
$e_{sd\sigma}$	−1.38111E+02	3.70841E+00	8.62354E−01	−1.97293E+02	−6.35844E+02
$f_{sd\sigma}$	2.56352E+01	−2.31465E−01	1.49029E−01	4.13772E+01	1.54736E+02
$\overline{f}_{sd\sigma}$	0.00000E+00	0.00000E+00	0.00000E+00	7.17648E−01	0.00000E+00
$g_{sd\sigma}$	9.15974E−01	6.95615E−01	7.63941E−01	1.09374E+00	1.24363E+00
$e_{pd\sigma}$	−7.63060E+01	−3.42076E+02	−1.98379E+00	−1.06522E+01	−1.66486E+00
$f_{pd\sigma}$	1.38687E+01	6.50911E+01	6.17796E−01	1.48098E+00	3.07154E−01
$\overline{f}_{pd\sigma}$	0.00000E+00	0.00000E+00	0.00000E+00	1.78179E−01	0.00000E+00
$g_{pd\sigma}$	8.79879E−01	1.03750E+00	7.89515E−01	8.98005E−01	6.91073E−01
$e_{pd\pi}$	−1.71792E−01	1.25909E+00	2.23528E+01	1.12385E+02	1.32243E+02
$f_{pd\pi}$	−3.17275E−01	−5.27343E−01	−5.63614E+00	−3.39863E+01	−4.33354E+01
$\overline{f}_{pd\pi}$	0.00000E+00	0.00000E+00	0.00000E+00	6.13082E−01	0.00000E+00
$g_{pd\pi}$	7.26150E−01	8.11349E−01	1.09404E+00	1.15426E+00	1.23322E+00
$e_{dd\sigma}$	−3.55884E+00	−3.25060E+01	−1.97035E−01	−5.40173E+02	−2.67754E+03
$f_{dd\sigma}$	8.69101E−01	8.16200E+00	3.64506E−01	1.59300E+02	6.84560E+02
$\overline{f}_{dd\sigma}$	0.00000E+00	0.00000E+00	0.00000E+00	−5.69928E+00	0.00000E+00
$g_{dd\sigma}$	7.21756E−01	9.54063E−01	8.52778E−01	1.27106E+00	1.43875E+00
$e_{dd\pi}$	1.67719E+01	−1.91191E+00	4.03560E−01	−2.08099E+01	−9.32516E−01
$f_{dd\pi}$	−4.08873E+00	9.91203E−02	−1.57338E+00	1.75627E+00	1.22212E−01
$\overline{f}_{dd\pi}$	0.00000E+00	0.00000E+00	0.00000E+00	−8.08524E−03	0.00000E+00
$g_{dd\pi}$	8.72084E−01	7.56434E−01	9.99799E−01	1.10078E+00	7.74043E−01
$e_{dd\delta}$	−5.68687E+01	3.04918E+01	3.44139E−01	−1.01318E+02	−4.20024E+01
$f_{dd\delta}$	1.99517E+01	−3.74711E+00	−2.87068E−02	1.94265E+01	8.89666E+00
$\overline{f}_{dd\delta}$	0.00000E+00	0.00000E+00	0.00000E+00	7.07164E−01	0.00000E+00
$g_{dd\delta}$	1.12436E+00	1.06028E+00	7.01862E−01	1.19473E+00	1.14476E+00

13

TABLE VIII. Tight-binding parameters (7-10) for Manganese, Iron, Cobalt, Nickel, and Copper. The equation numbers refer to the parametrization forms discussed in the text.

Parameter	Manganese	Iron	Cobalt	Nickel	Copper
On-Site Parameters Eqs. (7) and (9)					
λ	1.65076E+00	1.61592E+00	1.43580E+00	1.43847E+00	1.47292E+00
a_s	2.82713E−01	3.13939E−01	3.11786E−01	2.26020E−01	2.13398E−02
b_s	−2.44625E+01	−1.50341E+02	3.03424E+01	2.85451E+01	6.93939E+01
c_s	8.90173E+04	5.60132E+04	5.76787E+02	−1.40381E+02	−2.44787E+03
d_s	0.00000E+00	0.00000E+00	0.00000E+00	0.00000E+00	0.00000E+00
a_p	7.92094E−01	7.50228E−01	4.87203E−01	4.69576E−01	5.55994E−01
b_p	7.18208E+01	1.32173E+02	4.91535E+01	5.15499E+01	4.82152E+01
c_p	3.50298E+02	−4.83053E+03	−8.82385E+02	−1.16395E+03	−3.82848E+02
d_p	0.00000E+00	0.00000E+00	0.00000E+00	0.00000E+00	0.00000E+00
a_d	9.26905E−02	6.79136E−02	4.44373E−02	3.58969E−02	1.99140E−02
b_d	1.53106E+01	1.80488E+01	1.28650E+00	9.52349E−01	3.46551E−01
c_d	9.82070E+02	−1.71454E+03	1.44172E+01	−1.45504E+01	8.08263E+01
d_d	0.00000E+00	0.00000E+00	0.00000E+00	0.00000E+00	0.00000E+00
Hamiltonian Parameters Eq. (10)					
$e_{ss\sigma}$	3.42882E−01	4.55044E−01	−1.22054E+00	−1.38151E+00	−9.10328E+00
$f_{ss\sigma}$	−2.15584E−01	−1.21734E+00	−1.03624E−01	−1.20825E−01	5.17873E−01
$g_{ss\sigma}$	7.00302E−01	9.14315E−01	8.35761E−01	8.33833E−01	9.46662E−01
$e_{sp\sigma}$	5.68705E−01	8.72706E−01	1.99538E+00	2.08749E+00	3.10063E+00
$f_{sp\sigma}$	1.27669E−01	−2.65086E−03	5.04173E−02	8.44512E−02	−1.14987E−01
$g_{sp\sigma}$	6.66959E−01	6.78102E−01	8.17059E−01	8.07510E−01	8.16824E−01
$e_{pp\sigma}$	1.22039E+00	1.02661E+00	8.07087E−01	6.39053E−01	1.08944E+00
$f_{pp\sigma}$	−3.56575E−02	4.62878E−02	8.08439E−02	8.01499E−02	8.81043E−02
$g_{pp\sigma}$	6.20215E−01	6.49770E−01	6.77788E−01	6.63093E−01	7.44048E−01
$e_{pp\pi}$	−9.85276E+01	−3.61139E+01	−1.40024E−01	3.38998E−01	−3.47451E+00
$f_{pp\pi}$	3.70519E+01	8.18234E+00	−3.67928E−01	−3.32640E−01	4.87501E−01
$g_{pp\pi}$	1.25798E+00	1.17142E+00	8.87256E−01	8.46109E−01	8.54245E−01
$e_{sd\sigma}$	1.08489E+01	5.06145E−01	−1.26092E+00	−1.29152E+00	−2.32022E+00
$f_{sd\sigma}$	−2.59008E+00	−3.03407E−01	8.27292E−02	7.48429E−02	−3.15366E−02
$g_{sd\sigma}$	9.25004E−01	8.23582E−01	8.35781E−01	8.30637E−01	9.25016E−01
$e_{pd\sigma}$	5.60769E+00	3.62443E+00	−3.89270E−01	−4.18197E−01	−8.93442E−01
$f_{pd\sigma}$	−1.52163E+00	−1.20097E+00	2.21672E−03	−8.47911E−03	6.29553E−02
$g_{pd\sigma}$	8.50729E−01	8.70892E−01	7.15993E−01	6.98393E−01	7.37891E−01
$e_{pd\pi}$	−2.24611E+00	−1.23170E+00	3.93950E−01	9.56716E−02	−5.40577E+00
$f_{pd\pi}$	7.81059E−01	8.46862E−01	8.86907E−01	8.22286E−01	2.97343E+00
$g_{pd\pi}$	9.39607E−01	9.92416E−01	1.02442E+00	1.03137E+00	1.11838E+00
$e_{dd\sigma}$	−1.42480E+00	−1.30200E+00	−1.17737E+00	−1.14634E+00	−1.76354E+00
$f_{dd\sigma}$	6.29484E−03	9.13566E−02	−9.90018E−02	−7.89742E−02	1.19111E−01
$g_{dd\sigma}$	8.46043E−01	7.96761E−01	8.93869E−01	9.02008E−01	8.86270E−01
$e_{dd\pi}$	5.87164E+00	3.03158E+00	2.12933E+00	3.62103E+00	4.33011E+00
$f_{dd\pi}$	6.99707E−01	−2.29520E−01	6.30960E−01	4.97609E−01	1.60096E−01
$g_{dd\pi}$	1.07880E+00	9.29910E−01	1.04447E+00	1.07897E+00	1.08524E+00
$e_{dd\delta}$	−5.44863E+00	−2.42866E+00	−5.50043E−01	−1.36239E+00	8.61842E+00
$f_{dd\delta}$	−2.54667E+01	3.43810E−01	5.72799E−02	2.05114E−01	−3.97339E+00
$g_{dd\delta}$	1.45341E+00	1.01267E+00	8.74734E−01	9.76017E−01	1.29258E+00

			Overlap Parameters Eq. (10)		
$e_{ss\sigma}$	$-3.87663E+00$	$2.08692E+00$	$3.37736E+01$	$4.38609E+01$	$-4.62973E+00$
$f_{ss\sigma}$	$2.21239E+00$	$1.50952E+00$	$-6.02198E+00$	$-1.03415E+00$	$9.47334E+00$
$g_{ss\sigma}$	$8.66857E-01$	$9.38173E-01$	$1.14555E+00$	$1.17048E+00$	$1.14594E+00$
$e_{sp\sigma}$	$4.67005E+00$	$6.61325E+00$	$-3.59473E+00$	$-4.81962E+00$	$-7.76506E+00$
$f_{sp\sigma}$	$-1.26965E+00$	$-2.39708E+00$	$3.78546E-01$	$1.25105E-01$	$-7.02631E-01$
$g_{sp\sigma}$	$7.60452E-01$	$8.42816E-01$	$9.00865E-01$	$9.51048E-01$	$9.74543E-01$
$e_{pp\sigma}$	$9.65378E+00$	$7.79047E+00$	$-2.08360E-01$	$-3.93614E-01$	$-8.67146E-01$
$f_{pp\sigma}$	$-2.36416E+00$	$-2.24566E+00$	$-5.79196E-02$	$-6.04070E-02$	$2.08504E-03$
$g_{pp\sigma}$	$7.65420E-01$	$7.63650E-01$	$5.85309E-01$	$5.61312E-01$	$6.06850E-01$
$e_{pp\pi}$	$-4.63276E+00$	$-5.28179E+00$	$3.22718E-01$	$4.28633E-01$	$4.59109E-02$
$f_{pp\pi}$	$2.51612E+00$	$1.65817E+00$	$-8.25639E-03$	$2.84019E-03$	$5.34381E-02$
$g_{pp\pi}$	$9.21078E-01$	$8.02822E-01$	$6.14330E-01$	$5.81584E-01$	$6.65480E-01$
$e_{sd\sigma}$	$-1.25049E+03$	$-6.29774E+02$	$1.45688E+03$	$1.45970E+03$	$6.33227E+00$
$f_{sd\sigma}$	$2.77503E+02$	$1.71529E+02$	$-3.47915E+02$	$-3.44722E+02$	$1.08483E+00$
$g_{sd\sigma}$	$1.41062E+00$	$1.30437E+00$	$1.29390E+00$	$1.35652E+00$	$1.12244E+00$
$e_{pd\sigma}$	$-5.01714E-01$	$-3.79545E+00$	$-3.42786E+00$	$-3.98726E+00$	$-3.61230E+00$
$f_{pd\sigma}$	$-9.39420E-02$	$7.64597E-01$	$8.06002E-01$	$7.54214E-01$	$2.03040E-01$
$g_{pd\sigma}$	$7.58912E-01$	$8.45424E-01$	$7.56506E-01$	$7.69220E-01$	$9.56356E-01$
$e_{pd\pi}$	$1.30596E+02$	$1.21879E+02$	$-1.25831E+03$	$-1.47870E+03$	$-3.42670E+02$
$f_{pd\pi}$	$-3.89023E+01$	$-4.37850E+01$	$2.66826E+02$	$2.02738E+02$	$-5.22754E+01$
$g_{pd\pi}$	$1.16633E+00$	$1.33895E+00$	$1.44349E+00$	$1.46186E+00$	$1.51831E+00$
$e_{dd\sigma}$	$-1.50368E+03$	$-4.33297E+00$	$4.83403E+02$	$3.09179E+03$	$-1.72506E+03$
$f_{dd\sigma}$	$4.28271E+02$	$4.93980E+00$	$8.16729E+01$	$-3.49314E+02$	$4.47320E+02$
$g_{dd\sigma}$	$1.43291E+00$	$1.19874E+00$	$1.53933E+00$	$1.55682E+00$	$1.53713E+00$
$e_{dd\pi}$	$-1.18848E+00$	$-1.03641E+00$	$-1.07889E+00$	$-8.68984E-01$	$-6.49993E-01$
$f_{dd\pi}$	$2.24642E-02$	$1.93977E-01$	$1.24411E-02$	$6.12811E-02$	$-3.47252E-01$
$g_{dd\pi}$	$9.42798E-01$	$8.98115E-01$	$8.71866E-01$	$9.09043E-01$	$1.08398E+00$
$e_{dd\delta}$	$-6.61638E+01$	$4.62136E+00$	$-1.29889E+06$	$-4.61448E+05$	$2.17112E+01$
$f_{dd\delta}$	$1.62728E+01$	$-1.26354E+00$	$3.38458E+05$	$3.24162E+05$	$-4.38356E+00$
$g_{dd\delta}$	$1.15886E+00$	$1.05392E+00$	$1.97301E+00$	$2.01457E+00$	$1.18724E+00$

TABLE IX. Tight-binding parameters (7-10) for Strontium, Yttrium, Zirconium, Niobium, and Molybdenum. The equation numbers refer to the parametrization forms discussed in the text.

Parameter	Strontium	Yttrium	Zirconium	Niobium	Molybdenum
			On-Site Parameters Eqs. (7) and (9)		
λ	1.14372E+00	1.27304E+00	9.92096E−01	1.34109E+00	1.35071E+00
a_s	1.77264E−01	7.28123E−02	4.56862E−01	2.50727E−02	8.66826E−02
b_s	−1.31630E+01	9.32506E+00	−1.73980E+00	5.47470E+01	6.34195E+01
c_s	1.37270E+03	−4.92331E+02	−2.37835E+01	5.11141E+03	9.36509E+02
d_s	0.00000E+00	0.00000E+00	2.45157E+02	0.00000E+00	0.00000E+00
a_p	1.76186E−01	4.14728E−01	3.26016E−01	5.88564E−01	7.20981E−01
b_p	3.05689E+01	7.32116E+01	3.35603E+00	3.39986E+01	2.78880E+01
c_p	−5.40490E+02	−1.49339E+03	9.35236E+00	1.02038E+03	1.72325E+03
d_p	0.00000E+00	0.00000E+00	−3.24915E+01	0.00000E+00	0.00000E+00
a_d	2.41720E−01	2.07908E−01	1.09229E−01	1.38198E−01	1.02179E−01
b_d	1.87317E+00	−5.61629E+00	1.61113E+00	5.94294E+00	3.21725E+00
c_d	1.36064E+01	1.49923E+03	−6.46583E+00	1.48747E+02	1.61074E+02
d_d	0.00000E+00	0.00000E+00	1.91259E+01	0.00000E+00	0.00000E+00
			Hamiltonian Parameters Eq. (10)		
$e_{ss\sigma}$	1.01278E+02	7.72026E+00	5.69335E+00	−2.50992E+01	−7.59134E−01
$f_{ss\sigma}$	−1.60644E+01	−1.50419E+00	−1.57120E+00	−4.82208E−01	−2.42755E+00
$g_{ss\sigma}$	9.17082E−01	7.55938E−01	8.41753E−01	1.02758E+00	9.86587E−01
$e_{sp\sigma}$	−7.51014E+00	−1.39670E+00	−1.05737E+00	1.53790E+00	1.28784E+00
$f_{sp\sigma}$	1.26677E+00	3.59513E−01	3.53420E−01	9.57857E−02	2.35356E−01
$g_{sp\sigma}$	7.20485E−01	6.77441E−01	7.03266E−01	7.66846E−01	7.88792E−01
$e_{pp\sigma}$	−5.84498E−01	1.02671E+00	1.38018E+00	1.83668E+00	1.79716E+00
$f_{pp\sigma}$	1.04771E−01	−2.50961E−02	−8.27718E−02	−8.85229E−02	2.95321E−02
$g_{pp\sigma}$	5.41974E−01	5.44555E−01	5.42648E−01	6.16705E−01	6.71700E−01
$e_{pp\pi}$	3.78163E+07	9.35788E+09	4.92810E+00	−5.05098E+01	−2.22510E+01
$f_{pp\pi}$	−8.39757E+06	−1.43128E+09	1.43919E+01	6.76702E+00	1.82241E+00
$g_{pp\pi}$	1.72686E+00	2.03112E+00	1.27121E+00	1.15006E+00	1.05311E+00
$e_{sd\sigma}$	1.38973E+00	7.11340E−01	3.28602E−01	−8.21822E−01	−4.99283E−01
$f_{sd\sigma}$	−3.46441E−01	−1.55146E−01	−1.96275E−01	−6.54205E−03	3.80005E−02
$g_{sd\sigma}$	7.25100E−01	6.31695E−01	6.91552E−01	7.23214E−01	6.83391E−01
$e_{pd\sigma}$	7.31763E−01	7.96314E+00	5.43134E+00	−2.56118E−01	7.47595E−02
$f_{pd\sigma}$	−9.56001E−02	−1.33491E+00	−1.54334E+00	−1.54813E−02	−5.07410E−02
$g_{pd\sigma}$	5.59815E−01	7.43871E−01	8.11931E−01	6.02644E−01	6.03739E−01
$e_{pd\pi}$	3.58801E−01	7.43705E−02	−3.09334E−03	2.13205E−01	5.98715E−01
$f_{pd\pi}$	−3.27229E−02	3.88827E−03	2.47270E−03	−9.42484E−03	−2.22008E−02
$g_{pd\pi}$	5.12420E−01	6.34856E−01	5.14096E−01	6.92239E−01	7.39073E−01
$e_{dd\sigma}$	5.65896E+00	−1.28617E−02	−9.18974E−01	−1.53648E+00	−1.33254E+00
$f_{dd\sigma}$	−9.15043E−01	−4.00283E−02	−4.92553E−02	2.71430E−02	−8.68652E−03
$g_{dd\sigma}$	7.63696E−01	6.20401E−01	7.03930E−01	7.33958E−01	7.61081E−01
$e_{dd\pi}$	−3.38278E+00	9.61926E−01	1.05904E+00	2.78488E+00	3.48251E+00
$f_{dd\pi}$	9.46106E−01	1.89330E−01	1.63148E−01	5.06869E−02	−1.22045E−01
$g_{dd\pi}$	8.24676E−01	7.83094E−01	8.00179E−01	8.57695E−01	8.56524E−01
$e_{dd\delta}$	2.15625E+02	6.79257E+01	3.58548E+01	−3.45690E+01	−7.40531E−01
$f_{dd\delta}$	−3.46331E+01	−1.31752E+01	−8.49137E+00	−1.27137E+01	7.15057E−02
$g_{dd\delta}$	1.07240E+00	1.04788E+00	1.10660E+00	1.29063E+00	7.76694E−01

	Overlap Parameters Eq. (10)				
$e_{ss\sigma}$	1.32808E+01	-1.32457E+00	-1.30200E+00	3.19400E$-$01	3.05256E+02
$f_{ss\sigma}$	-1.27851E+00	2.71913E+00	2.30501E+00	-6.04851E$-$04	-3.52015E+01
$g_{ss\sigma}$	7.07779E$-$01	8.08101E$-$01	8.99383E$-$01	7.44630E$-$01	1.26105E+00
$e_{sp\sigma}$	3.73826E+04	5.24175E+02	4.30489E+02	-1.98466E+03	1.32679E+03
$f_{sp\sigma}$	-5.69590E+03	-1.01379E+02	-1.10041E+02	1.59179E+02	-4.00480E+02
$g_{sp\sigma}$	1.16729E+00	1.02133E+00	1.12375E+00	1.34929E+00	1.33379E+00
$e_{pp\sigma}$	6.30614E+02	2.32538E+01	8.90408E$-$01	4.02407E+00	1.10983E+00
$f_{pp\sigma}$	-1.01825E+02	-4.94018E+00	1.00989E+00	-4.80091E$-$03	-3.32012E$-$01
$g_{pp\sigma}$	9.44726E$-$01	8.01543E$-$01	9.08075E$-$01	8.84240E$-$01	6.46625E$-$01
$e_{pp\pi}$	-1.69469E+02	-8.46463E+10	2.23043E+01	-6.84291E$-$01	-1.58174E+00
$f_{pp\pi}$	2.77774E+01	1.43007E+10	1.29974E+01	2.91908E$-$01	3.04289E$-$01
$g_{pp\pi}$	8.77067E$-$01	2.05732E+00	1.20161E+00	2.75732E+00	6.45588E$-$01
$e_{sd\sigma}$	-6.09261E+02	-1.90620E+02	-8.21444E+02	2.67689E+00	4.31740E$-$01
$f_{sd\sigma}$	9.90033E+01	3.84507E+01	1.91013E+02	2.37409E$-$01	1.31467E$-$01
$g_{sd\sigma}$	9.57395E$-$01	9.65863E$-$01	1.14321E+00	8.09336E$-$01	6.84817E$-$01
$e_{pd\sigma}$	-1.65574E+02	1.29405E+00	0.00000E+00	5.73767E$-$01	4.03350E$-$01
$f_{pd\sigma}$	2.72554E+01	-9.61853E$-$02	0.00000E+00	-3.90244E$-$02	-3.04020E$-$02
$g_{pd\sigma}$	8.68471E$-$01	5.37486E$-$01	1.00000E+00	5.08340E$-$01	3.85790E$-$01
$e_{pd\pi}$	6.84374E+00	6.14466E+01	3.66168E+01	6.15636E$-$01	4.48953E$-$01
$f_{pd\pi}$	-1.43215E+00	-1.25963E+01	-9.03817E+00	-2.16620E$-$01	-1.59315E$-$01
$g_{pd\pi}$	7.16925E$-$01	9.14935E$-$01	9.83872E$-$01	7.64261E$-$01	7.32118E$-$01
$e_{dd\sigma}$	-1.39363E+01	-3.24712E+01	-4.84660E+01	-3.43653E$-$01	2.47289E$-$01
$f_{dd\sigma}$	2.65537E+00	6.51211E+00	1.17934E+01	1.55909E$-$01	-1.72562E$-$02
$g_{dd\sigma}$	7.39857E$-$01	8.29440E$-$01	1.02194E+00	6.65039E$-$01	4.36793E$-$01
$e_{dd\pi}$	1.37850E+02	1.44898E+02	1.56704E+02	-1.88524E+00	-7.55891E$-$01
$f_{dd\pi}$	-2.52973E+01	-2.91678E+01	-3.85906E+01	2.56521E$-$02	5.55713E$-$02
$g_{dd\pi}$	9.08764E$-$01	9.71214E$-$01	1.10151E+00	7.54927E$-$01	6.03483E$-$01
$e_{dd\delta}$	-3.88013E+02	8.80037E+01	-1.14800E+01	2.48974E$-$01	1.21646E+00
$f_{dd\delta}$	8.01182E+01	4.30951E+00	5.38231E+00	-2.44331E$-$02	6.30985E$-$03
$g_{dd\delta}$	1.10480E+00	1.15554E+00	1.11935E+00	5.59223E$-$01	8.82482E$-$01

TABLE X. Tight-binding parameters (7-10) for Technetium, Ruthenium, Rhodium, Palladium, and Silver. The equation numbers refer to the parametrization forms discussed in the text.

Parameter	Technetium	Ruthenium	Rhodium	Palladium	Silver
	On-Site Parameters Eqs. (7) and (9)				
λ	1.35605E+00	1.34253E+00	1.34056E+00	1.27733E+00	1.22495E+00
a_s	1.56969E−01	8.93160E−02	9.12651E−02	9.21895E−02	1.71377E−01
b_s	4.96528E+01	4.12031E+01	4.48975E+01	2.66437E+01	8.37704E+00
c_s	6.87483E+02	1.29943E+03	8.96404E+02	2.45427E+02	−1.77374E+01
d_s	0.00000E+00	0.00000E+00	0.00000E+00	0.00000E+00	0.00000E+00
a_p	7.27706E−01	6.70655E−01	6.20365E−01	5.05324E−01	6.05047E−01
b_p	2.33596E+01	4.08917E+01	4.44309E+01	3.52846E+01	1.23316E+01
c_p	1.80513E+03	3.65045E+01	−7.16816E+01	−1.73870E+02	2.00392E+01
d_p	0.00000E+00	0.00000E+00	0.00000E+00	0.00000E+00	0.00000E+00
a_d	8.87546E−02	6.47777E−02	4.90478E−02	2.77484E−02	4.32432E−03
b_d	1.68547E+00	1.15434E+00	7.99566E−01	2.34504E−01	8.54569E−02
c_d	9.14454E+01	4.02940E+01	−1.33019E+01	−1.16871E+01	−5.98728E−01
d_d	0.00000E+00	0.00000E+00	0.00000E+00	0.00000E+00	0.00000E+00
	Hamiltonian Parameters Eq. (10)				
$e_{ss\sigma}$	−2.42325E−01	−1.06826E+01	−1.03870E+01	−9.65803E+00	−3.02245E+00
$f_{ss\sigma}$	−2.35701E+00	−5.19162E−01	0.00000E+00	−6.58566E−02	2.82192E−01
$g_{ss\sigma}$	9.90587E−01	9.98652E−01	9.74343E−01	9.65567E−01	7.53400E−01
$e_{sp\sigma}$	1.32706E+00	5.36202E+00	7.11658E+00	6.92889E+00	2.46216E+00
$f_{sp\sigma}$	2.33454E−01	2.42663E−02	0.00000E+00	−8.05132E−03	−6.72462E−02
$g_{sp\sigma}$	7.91274E−01	8.79989E−01	9.06080E−01	8.93397E−01	7.93558E−01
$e_{pp\sigma}$	1.67313E+00	3.00393E+00	2.61732E+00	3.10178E+00	−1.52677E+01
$f_{pp\sigma}$	7.40188E−03	1.98109E−02	0.00000E+00	−3.64082E−03	4.55095E+00
$g_{pp\sigma}$	6.65741E−01	7.26256E−01	7.04652E−01	7.29562E−01	8.98600E−01
$e_{pp\pi}$	−2.05304E+01	−8.52581E−02	−9.15155E−02	−8.63018E−02	−4.24238E+02
$f_{pp\pi}$	2.07455E+00	−2.22726E−03	0.00000E+00	−3.08492E−03	−2.33808E+02
$g_{pp\pi}$	1.03629E+00	5.41216E−01	5.24756E−01	5.72566E−01	1.61153E+00
$e_{sd\sigma}$	−6.50753E−01	−1.63451E+00	−4.27539E+00	−1.79028E+00	−1.12908E+00
$f_{sd\sigma}$	5.67702E−02	−9.54826E−02	0.00000E+00	−1.40935E−02	9.41454E−02
$g_{sd\sigma}$	6.57744E−01	8.93940E−01	9.40417E−01	8.55849E−01	7.06503E−01
$e_{pd\sigma}$	−2.26321E−02	−5.08077E−01	−6.91759E−01	−7.13093E−01	3.72317E+00
$f_{pd\sigma}$	−5.91240E−02	6.17604E−04	0.00000E+00	−2.66134E−03	−1.48971E+00
$g_{pd\sigma}$	6.24648E−01	6.66661E−01	6.72844E−01	6.91813E−01	9.00056E−01
$e_{pd\pi}$	5.73187E−01	3.33146E−01	1.05800E−01	2.53192E−01	2.76295E+00
$f_{pd\pi}$	−3.81543E−02	−3.86754E−03	0.00000E+00	−2.89608E−03	1.87799E−01
$g_{pd\pi}$	7.46410E−01	7.10996E−01	6.16605E−01	7.19375E−01	1.02993E+00
$e_{dd\sigma}$	−1.32507E+00	−2.47448E+00	−2.24220E+00	−2.00840E+00	−2.83314E+00
$f_{dd\sigma}$	−9.81573E−03	−4.63223E−02	0.00000E+00	−1.50392E−02	−6.41209E−01
$g_{dd\sigma}$	7.70176E−01	8.54974E−01	8.45401E−01	8.53056E−01	9.78615E−01
$e_{dd\pi}$	4.14667E+00	4.17666E+00	5.70876E+00	8.17277E+00	9.65404E+00
$f_{dd\pi}$	−1.30743E−01	1.94391E−02	0.00000E+00	−8.64748E−02	−8.32773E−01
$g_{dd\pi}$	8.91789E−01	9.34693E−01	9.82160E−01	1.02752E+00	1.01612E+00
$e_{dd\delta}$	−9.72649E−01	5.28412E+00	−1.68497E+00	−2.34604E+00	2.59720E+01
$f_{dd\delta}$	1.30476E−01	−2.14644E+00	0.00000E+00	3.25537E−01	−1.38837E+01
$g_{dd\delta}$	7.84398E−01	1.11033E+00	1.04917E+00	9.76385E−01	1.36049E+00

			Overlap Parameters Eq. (10)		
$e_{ss\sigma}$	2.97103E+02	1.27671E+01	−1.80513E+03	1.17693E+04	5.19751E+00
$f_{ss\sigma}$	−3.76325E+01	8.94019E−02	0.00000E+00	−5.39387E+02	−1.81289E−01
$g_{ss\sigma}$	1.25946E+00	1.95994E+00	2.21069E+00	1.62329E+00	8.60426E−01
$e_{sp\sigma}$	1.44349E+03	−1.05981E+04	−1.12235E+04	−1.53705E+04	−2.28701E+00
$f_{sp\sigma}$	−3.79690E+02	−2.72224E+02	0.00000E+00	2.32248E+03	−1.61325E−01
$g_{sp\sigma}$	1.30455E+00	1.62336E+00	1.61109E+00	1.50175E+00	7.74383E−01
$e_{pp\sigma}$	7.57425E−01	1.58799E+01	−5.49048E+00	2.19627E+00	−3.78981E+00
$f_{pp\sigma}$	−2.94235E−01	−3.08498E+00	0.00000E+00	−7.10592E−01	−5.15424E−01
$g_{pp\sigma}$	6.58479E−01	9.91155E−01	1.08039E+00	8.19278E−01	9.06381E−01
$e_{pp\pi}$	−1.48293E+00	1.40686E+01	−1.40201E−02	−6.16862E−01	−5.78210E+03
$f_{pp\pi}$	2.88300E−01	−9.07707E−04	0.00000E+00	1.33749E−01	1.25726E+03
$g_{pp\pi}$	6.50767E−01	1.98112E+00	1.73125E+00	7.11976E−01	1.36538E+00
$e_{sd\sigma}$	7.28149E−01	2.66680E−01	−2.09986E+00	−1.37473E+01	2.87589E−01
$f_{sd\sigma}$	7.43369E−02	1.19878E−01	0.00000E+00	2.65050E−01	3.25719E−02
$g_{sd\sigma}$	6.87723E−01	7.69449E−01	1.16939E+00	1.07480E+00	7.24168E−01
$e_{pd\sigma}$	4.34355E−01	−1.54734E+03	−4.40618E+02	−1.25579E+02	−1.24324E+01
$f_{pd\sigma}$	−3.40641E−02	−2.04299E+03	0.00000E+00	−3.20496E+01	1.90544E+00
$g_{pd\sigma}$	4.18094E−01	1.95694E+00	1.38332E+00	1.25500E+00	9.52608E−01
$e_{pd\pi}$	5.61187E−01	−3.96833E−01	−5.68639E+01	−7.57995E+02	−1.79373E+00
$f_{pd\pi}$	−1.39188E−01	5.43342E−02	0.00000E+00	−3.66651E+00	2.67272E−01
$g_{pd\pi}$	7.25597E−01	5.68958E−01	1.21849E+00	1.37921E+00	7.56593E−01
$e_{dd\sigma}$	3.23273E−01	−4.42200E+00	2.38357E+00	3.35457E+01	1.43164E+01
$f_{dd\sigma}$	1.72275E−02	2.03106E+00	0.00000E+00	−6.81529E−01	−2.47557E+00
$g_{dd\sigma}$	6.14412E−01	9.65997E−01	8.81490E−01	1.14453E+00	9.44667E−01
$e_{dd\pi}$	−6.98334E−01	−4.84435E+00	−2.32596E+01	−1.50866E+01	−7.84762E+00
$f_{dd\pi}$	5.95975E−02	−4.04300E−01	0.00000E+00	1.44912E−01	2.94062E−01
$g_{dd\pi}$	6.29126E−01	1.02395E+00	1.12774E+00	1.10093E+00	1.04716E+00
$e_{dd\delta}$	1.39075E+00	1.33535E+04	5.83229E+03	1.05067E+03	5.03416E+01
$f_{dd\delta}$	−5.99108E−02	4.97401E+03	0.00000E+00	2.44615E+01	−7.80465E+00
$g_{dd\delta}$	9.31751E−01	1.76428E+00	1.60401E+00	1.47110E+00	1.15950E+00

TABLE XI. Tight-binding parameters (7-10) for Barium, Hafnium, Tantalum, and Tungsten. The equation numbers refer to the parametrization forms discussed in the text.

Parameter	Barium	Hafnium	Tantalum	Tungsten
	On-Site Parameters Eqs. (7) and (9)			
λ	1.11634E+00	1.19630E+00	1.27675E+00	1.32674E+00
a_s	1.50138E−01	9.10131E−01	3.19292E−01	4.33397E−01
b_s	−1.53745E+01	5.29294E+00	3.66642E−01	1.42840E+00
c_s	1.56954E+03	5.04222E+02	4.42664E+02	4.00732E+02
d_s	0.00000E+00	4.95952E+02	0.00000E+00	0.00000E+00
a_p	1.28894E−01	4.65965E−01	3.59226E−01	4.27055E−01
b_p	2.72310E+01	2.94282E+01	5.38397E+01	8.21465E+01
c_p	1.64446E+03	−3.86257E+02	−4.57578E+02	−1.13769E+03
d_p	0.00000E+00	1.23293E+03	0.00000E+00	0.00000E+00
a_d	1.82919E−01	2.63519E−01	1.61383E−01	2.17265E−01
b_d	9.59617E−01	4.75514E+00	2.74648E+00	−2.63465E+00
c_d	−9.73190E+01	4.74879E+01	1.22440E+02	3.23869E+02
d_d	0.00000E+00	−7.45384E+02	0.00000E+00	0.00000E+00
	Hamiltonian Parameters Eq. (10)			
$e_{ss\sigma}$	1.07625E+02	9.13877E+00	−3.81526E−01	4.59797E+00
$f_{ss\sigma}$	−1.54756E+01	1.54875E+00	0.00000E+00	−1.06279E+00
$g_{ss\sigma}$	8.83547E−01	9.83725E−01	5.91644E−01	7.81632E−01
$e_{sp\sigma}$	−8.15023E+00	−9.83656E−01	1.07250E+00	−2.71873E−02
$f_{sp\sigma}$	1.18680E+00	4.73735E−01	0.00000E+00	4.18002E−01
$g_{sp\sigma}$	7.05573E−01	6.25311E−01	6.60713E−01	7.28960E−01
$e_{pp\sigma}$	−7.65354E−01	−3.62500E+00	1.96224E+00	1.04741E+00
$f_{pp\sigma}$	1.11812E−01	1.28779E+00	0.00000E+00	1.14611E+00
$g_{pp\sigma}$	5.22978E−01	7.57257E−01	6.54733E−01	7.99230E−01
$e_{pp\pi}$	−4.49769E+08	−1.86311E+00	−1.25096E+02	4.35429E+01
$f_{pp\pi}$	6.24773E+07	1.55799E−01	0.00000E+00	−7.09146E+00
$g_{pp\pi}$	1.72686E+00	9.06562E−01	1.33474E+00	1.10993E+00
$e_{sd\sigma}$	1.51803E+00	3.28266E+00	−5.39923E−01	−7.48675E−01
$f_{sd\sigma}$	−3.17484E−01	−1.20838E+00	0.00000E+00	−5.87424E−02
$g_{sd\sigma}$	7.01455E−01	7.79418E−01	7.12949E−01	7.15275E−01
$e_{pd\sigma}$	1.38944E+00	1.08653E−01	−1.52215E−01	5.22978E+00
$f_{pd\sigma}$	−1.70619E−01	−5.64207E−01	0.00000E+00	−1.54532E+00
$g_{pd\sigma}$	5.57474E−01	7.13632E−01	5.71662E−01	8.11224E−01
$e_{pd\pi}$	3.19179E−01	−3.46529E+00	3.74952E−01	−3.92986E+01
$f_{pd\pi}$	−3.37340E−02	9.67868E−01	0.00000E+00	7.65413E+00
$g_{pd\pi}$	6.20946E−01	1.05238E+00	6.53815E−01	1.03638E+00
$e_{dd\sigma}$	9.48343E+00	−2.15888E−01	−1.30670E+00	−6.77733E−01
$f_{dd\sigma}$	−1.44518E+00	−2.80122E−01	0.00000E+00	−5.81468E−01
$g_{dd\sigma}$	7.49400E−01	7.11762E−01	7.25180E−01	8.48777E−01
$e_{dd\pi}$	−2.85791E+00	1.71474E+00	1.12618E+00	5.95483E+00
$f_{dd\pi}$	8.93926E−01	5.62278E−01	0.00000E+00	−3.94918E−01
$g_{dd\pi}$	8.11059E−01	9.14855E−01	7.22741E−01	8.85080E−01
$e_{dd\delta}$	1.87063E+02	1.33656E+01	−2.46591E+00	−3.01847E+01
$f_{dd\delta}$	−2.53043E+01	6.13820E−01	0.00000E+00	2.76809E+00
$g_{dd\delta}$	9.83611E−01	1.07864E+00	9.37069E−01	1.19769E+00

	Overlap Parameters Eq. (10)			
$e_{ss\sigma}$	1.83722E+01	1.18231E+01	4.95296E+00	-1.01186E+03
$f_{ss\sigma}$	-1.43245E+00	2.96234E+00	0.00000E+00	2.64629E+02
$g_{ss\sigma}$	7.19225E$-$01	9.46583E$-$01	8.52620E$-$01	1.25307E+00
$e_{sp\sigma}$	4.44201E+04	1.72009E+00	-4.73578E+02	-3.78579E$-$01
$f_{sp\sigma}$	-6.40797E+03	-2.35586E+00	0.00000E+00	-1.09561E$-$01
$g_{sp\sigma}$	1.14903E+00	8.62716E$-$01	1.31345E+00	7.26138E$-$01
$e_{pp\sigma}$	-7.35150E+02	1.54031E+01	-1.11120E$-$01	-7.94937E+01
$f_{pp\sigma}$	-1.22332E+02	-4.49554E+00	0.00000E+00	1.75411E+01
$g_{pp\sigma}$	1.09529E+00	9.33910E$-$01	1.29482E+00	1.12795E+00
$e_{pp\pi}$	-2.62750E+01	2.80432E+01	1.70576E+04	2.84202E+02
$f_{pp\pi}$	1.77696E+01	-2.12441E+00	0.00000E+00	-4.98337E+01
$g_{pp\pi}$	9.13209E$-$01	1.07278E+00	2.02320E+00	1.15218E+00
$e_{sd\sigma}$	-5.54362E+02	6.14493E+00	2.10081E+00	1.86528E+01
$f_{sd\sigma}$	8.25381E+01	-1.61559E+00	0.00000E+00	1.45875E+01
$g_{sd\sigma}$	9.13548E$-$01	1.28745E+00	7.03679E$-$01	1.19625E+00
$e_{pd\sigma}$	-1.98494E+02	7.95537E+00	1.08905E+00	-2.31625E+01
$f_{pd\sigma}$	3.13853E+01	-2.35268E+00	0.00000E+00	1.40867E+01
$g_{pd\sigma}$	8.78901E$-$01	9.07766E$-$01	6.11045E$-$01	1.14689E+00
$e_{pd\pi}$	9.42421E+00	1.55087E+00	-3.47807E$-$02	-2.20429E+01
$f_{pd\pi}$	-1.77293E+00	-4.88415E$-$01	0.00000E+00	1.06219E+00
$g_{pd\pi}$	6.93194E$-$01	8.56422E$-$01	4.74891E$-$01	1.06161E+00
$e_{dd\sigma}$	-2.28081E+01	3.36607E+01	2.24207E$-$01	-4.53347E+01
$f_{dd\sigma}$	3.96599E+00	-8.74169E+00	0.00000E+00	1.19568E+01
$g_{dd\sigma}$	7.50292E$-$01	1.20766E+00	4.92531E$-$01	1.03146E+00
$e_{dd\pi}$	1.30794E+02	-1.26460E+01	-1.83289E+00	5.24024E+02
$f_{dd\pi}$	-2.48946E+01	1.05554E+00	0.00000E+00	-1.33112E+02
$g_{dd\pi}$	8.94081E$-$01	9.07237E$-$01	7.62263E$-$01	1.22976E+00
$e_{dd\delta}$	1.07020E+04	6.04877E+01	4.42902E$-$01	-1.38362E+01
$f_{dd\delta}$	-1.18878E+03	-5.00466E+00	0.00000E+00	6.70560E+00
$g_{dd\delta}$	1.17919E+00	1.09546E+00	7.43396E$-$01	1.19251E+00

TABLE XII. Tight-binding parameters (7-10) for Rhenium, Osmium, Iridium, Platinum, and Gold. The equation numbers refer to the parametrization forms discussed in the text.

Parameter	Rhenium	Osmium	Iridium	Platinum	Gold
			On-Site Parameters Eqs. (7) and (9)		
λ	1.41690E+00	1.43787E+00	1.48862E+00	1.48637E+00	1.37357E+00
a_s	1.25774E−01	2.19235E−01	2.58676E−01	5.83156E−03	9.52842E−02
b_s	4.32410E+01	2.32773E+01	8.99491E+01	2.05116E+02	4.03569E+01
c_s	−2.65528E+03	−1.49716E+02	−5.38470E+03	−2.04105E+04	−3.05963E+03
d_s	0.00000E+00	0.00000E+00	0.00000E+00	0.00000E+00	0.00000E+00
a_p	6.08286E−01	7.15539E−01	6.49919E−01	8.17823E−01	5.75191E−01
b_p	5.39672E+01	7.50020E+01	1.26272E+02	5.89750E+01	1.40526E+01
c_p	5.88296E+03	4.09052E+03	9.65187E+03	1.12390E+04	−8.66127E+00
d_p	0.00000E+00	0.00000E+00	0.00000E+00	0.00000E+00	0.00000E+00
a_d	1.15150E−01	9.48499E−02	5.69648E−02	4.98288E−02	2.16623E−02
b_d	3.02548E+00	−8.99667E−01	2.78655E−01	−4.47348E+00	1.02921E+00
c_d	5.66609E+02	5.91858E+02	1.80727E+02	6.15745E+02	−3.77491E+01
d_d	0.00000E+00	0.00000E+00	0.00000E+00	0.00000E+00	0.00000E+00
			Hamiltonian Parameters Eq. (10)		
$e_{ss\sigma}$	1.53798E+01	9.56167E+00	−1.25321E+00	−1.38285E+00	−3.80906E+00
$f_{ss\sigma}$	−3.57908E+00	−3.86825E+00	−1.06638E−01	−1.20674E−01	−4.38467E−01
$g_{ss\sigma}$	8.70774E−01	9.68851E−01	8.16908E−01	8.13945E−01	9.08853E−01
$e_{sp\sigma}$	9.12123E−01	7.69439E−01	1.84853E+00	1.83354E+00	1.15267E+00
$f_{sp\sigma}$	2.73036E−01	2.88606E−01	5.84833E−01	5.86127E−01	−1.43508E−02
$g_{sp\sigma}$	7.96353E−01	7.87669E−01	8.45321E−01	8.45134E−01	6.80672E−01
$e_{pp\sigma}$	2.22720E+00	1.60364E+00	1.10831E+00	1.26085E+00	−3.33685E+00
$f_{pp\sigma}$	2.72264E−01	4.70495E−01	1.03256E+00	1.03890E+00	1.05126E+00
$g_{pp\sigma}$	8.00001E−01	7.56961E−01	8.31571E−01	8.31225E−01	7.97642E−01
$e_{pp\pi}$	−1.26133E+01	9.34510E−01	1.91089E+02	2.05176E+02	4.78096E+02
$f_{pp\pi}$	−2.52237E−01	−4.41535E−01	−4.16812E+01	−3.96380E+01	−1.14000E+02
$g_{pp\pi}$	1.00962E+00	8.42600E−01	1.13693E+00	1.13165E+00	1.39758E+00
$e_{sd\sigma}$	−6.80815E−01	−1.20891E+00	−3.02142E+00	−2.89295E+00	−2.73600E+00
$f_{sd\sigma}$	5.60338E−02	1.00979E−01	3.22373E−01	2.44946E−01	2.21303E−01
$g_{sd\sigma}$	5.97382E−01	6.87352E−01	7.78863E−01	7.98201E−01	7.86845E−01
$e_{pd\sigma}$	−3.89432E−01	2.91611E−01	1.91293E+00	1.58551E+00	3.72568E+00
$f_{pd\sigma}$	−5.46612E−02	−1.78914E−01	−6.34580E−01	−6.94619E−01	−1.48066E+00
$g_{pd\sigma}$	7.33599E−01	7.31519E−01	8.28540E−01	8.07844E−01	8.83740E−01
$e_{pd\pi}$	6.87010E−01	8.49872E−01	1.12973E+00	8.60594E−01	−4.98763E+00
$f_{pd\pi}$	7.97327E−02	9.73177E−02	−5.49139E−02	−3.28210E−02	1.61999E+00
$g_{pd\pi}$	8.44466E−01	8.65611E−01	8.13738E−01	8.59014E−01	9.86804E−01
$e_{dd\sigma}$	−2.05734E+00	−1.84915E+00	−1.69848E+00	−1.75160E+00	−3.20091E+00
$f_{dd\sigma}$	−7.81615E−02	−9.78854E−02	−3.17559E−01	−3.17277E−01	2.80249E−01
$g_{dd\sigma}$	8.23143E−01	8.19999E−01	8.67395E−01	8.74769E−01	8.01174E−01
$e_{dd\pi}$	4.93020E+00	4.81023E+00	5.45277E+00	7.04207E+00	1.28200E+01
$f_{dd\pi}$	−8.00019E−02	−6.04252E−02	−3.36078E−02	−3.61063E−01	−1.27555E+00
$g_{dd\pi}$	8.98430E−01	9.11958E−01	9.38700E−01	9.55738E−01	9.96619E−01
$e_{dd\delta}$	−3.42830E+00	−2.11302E+00	−8.81866E−01	−1.19555E+00	1.54046E+03
$f_{dd\delta}$	3.08896E−01	1.76612E−01	1.01129E−01	1.68460E−01	−3.98715E+02
$g_{dd\delta}$	9.39165E−01	9.26725E−01	8.09760E−01	8.73327E−01	1.50519E+00

	Overlap Parameters Eq. (10)				
$e_{ss\sigma}$	-7.65992E+02	3.42921E+01	8.03977E+00	8.48032E+00	5.49189E+00
$f_{ss\sigma}$	2.20348E+02	-1.86163E+00	-1.31689E+00	-1.21344E+00	-5.81247E$-$01
$g_{ss\sigma}$	1.23551E+00	1.05666E+00	8.31100E$-$01	8.73589E$-$01	8.01636E$-$01
$e_{sp\sigma}$	2.45545E+03	-9.08968E+01	1.86281E+03	2.07666E+03	1.47488E+00
$f_{sp\sigma}$	-5.52012E+02	7.58654E+00	-5.45115E+02	-4.87117E+02	-1.70493E+00
$g_{sp\sigma}$	1.33722E+00	1.12351E+00	1.41339E+00	1.42828E+00	8.83162E$-$01
$e_{pp\sigma}$	-1.87751E+01	2.24577E$-$01	-4.81893E+02	-1.59104E+04	4.39256E+00
$f_{pp\sigma}$	-3.24397E+00	-8.87977E$-$02	-3.77409E+03	3.39007E+03	-1.14950E+00
$g_{pp\sigma}$	1.13916E+00	1.00155E+00	1.64783E+00	1.46845E+00	7.63723E$-$01
$e_{pp\pi}$	-3.01308E+00	4.66106E$-$01	7.01099E+02	-4.68566E+02	7.25807E$-$01
$f_{pp\pi}$	9.07266E$-$02	-2.97036E$-$02	-1.37636E+02	1.29049E+02	2.46341E$-$04
$g_{pp\pi}$	9.40898E$-$01	1.00008E+00	1.22085E+00	1.24801E+00	5.60606E$-$01
$e_{sd\sigma}$	6.58787E+00	-2.99936E$-$01	-1.23356E+00	-1.88028E+00	7.82884E+02
$f_{sd\sigma}$	5.25043E$-$01	6.59351E$-$01	4.96759E$-$01	4.33068E$-$01	-5.72404E+01
$g_{sd\sigma}$	9.32724E$-$01	7.95665E$-$01	7.36238E$-$01	7.48675E$-$01	1.35691E+00
$e_{pd\sigma}$	1.51040E+00	8.30255E$-$01	8.06687E$-$01	1.40632E$-$01	-1.59724E+01
$f_{pd\sigma}$	8.03788E$-$02	-6.94731E$-$02	-5.95955E$-$02	-1.08624E$-$02	3.65486E+00
$g_{pd\sigma}$	6.91649E$-$01	5.55561E$-$01	5.19117E$-$01	4.30680E$-$01	9.11474E$-$01
$e_{pd\pi}$	2.77713E+00	-1.45265E$-$01	-1.75883E+00	-2.32135E+00	-2.09876E+03
$f_{pd\pi}$	-5.08983E$-$01	-7.56943E$-$03	3.88548E$-$01	3.29353E$-$01	3.24572E+02
$g_{pd\pi}$	7.90651E$-$01	1.00011E+00	8.31669E$-$01	7.81550E$-$01	1.36489E+00
$e_{dd\sigma}$	2.08835E$-$01	-2.14857E+01	8.54708E$-$01	7.85665E$-$01	1.16130E+04
$f_{dd\sigma}$	7.98506E$-$02	8.12810E+00	-7.41190E$-$03	-4.01901E$-$02	-6.39800E+02
$g_{dd\sigma}$	6.28966E$-$01	1.04606E+00	6.96686E$-$01	7.02103E$-$01	1.57650E+00
$e_{dd\pi}$	-1.45230E+00	-1.80998E+00	-3.39400E+00	-3.26443E+00	-2.12382E+00
$f_{dd\pi}$	1.43697E$-$01	1.38350E$-$01	-2.60852E$-$02	5.45025E$-$02	2.85113E$-$01
$g_{dd\pi}$	6.78231E$-$01	7.61277E$-$01	8.93060E$-$01	9.05926E$-$01	7.62212E$-$01
$e_{dd\delta}$	9.19531E$-$02	1.62148E$-$01	2.14814E+02	1.65627E+03	2.32941E+01
$f_{dd\delta}$	7.24211E$-$02	-8.40874E$-$03	1.62838E+01	-2.95917E+02	-4.22448E+00
$g_{dd\delta}$	8.78356E$-$01	7.18986E$-$01	1.40077E+00	1.32876E+00	1.01272E+00

[1] R. E. Cohen, M. J. Mehl, and D. A. Papaconstantopoulos, Phys. Rev. B, **50** 14694, (1994).

[2] M. J. Mehl, J. E. Osburn, D. A. Papaconstantopoulos, and B. M. Klein, Phys. Rev. B, **41**, 10311 (1990); errata Phys. Rev. B, **42**, 5362 (1991).

[3] M. J. Mehl, J. E. Osburn, D. A. Papaconstantopoulos, and B. M. Klein, Mat. Res. Soc. Symp. Proc. **186** 227 (1991).

[4] M. J. Mehl, Phys. Rev. B, **47**, 2493 (1993).

[5] M. J. Mehl, B. M. Klein, and D. A. Papaconstantopoulos, "First-Principles Calculation of Elastic Properties," in *Intermetallic Compounds: Principles and Applications*, ed. J. H. Westbrook and R. L. Fleischer (London: John Wiley & Sons Ltd., 1994), Vol. 1.

[6] P. Hohenberg and W. Kohn, Phys. Rev. **136**, B864 (1964).

[7] W. Kohn and L. J. Sham, Phys. Rev. **140**, A1133 (1965).

[8] M. J. Gillan, J. Phys. Condens. Mat., **1**, 689 (1989).

[9] M. M. Sigalas and D. A. Papaconstantopoulos, Phys. Rev. B, **49**, 1574 (1994).

[10] C. H. Xu, C. Z. Wang, C. T. Chan, and K. M. Ho, J. Phys. Condens. Matt., **4**, 6047 (1992).

[11] L. Goodwin, A. J. Skinner, and D. G. Pettifor, Europhysics Letters, **9**, 701 (1989).

[12] A.E. Carlsson, Phys. Rev. B, **44**, 6590 (1991).

[13] A.P. Sutton, M.W. Finnis, D.G. Pettifor, and Y. Ohta, J. Phys. C, **21** 35 (1988).

[14] J.L. Mercer, Jr. and M.Y. Chou, Phys. Rev. B, **47**, 9366 (1993).

[15] M. Menon, J. Connolly, N. Lathiotakis, and A. Andriotis, Phys. Rev. B **50**, 8903 (1994).

[16] N.N. Lathiotakis, A.N. Andriotis, M. Menon, and J. Connolly, Europhysics Letters **29**, 135 (1995).

[17] J.C. Slater and G.F. Koster, Phys. Rev. **94**, 1498 (1954).

[18] J.L. Mercer, Jr. and M.Y. Chou, Phys. Rev. B, **49**, 8506 (1994).

[19] D. A. Papaconstantopoulos, *Handbook of Electronic Structure of Elemental Solids* (New York, NY: Plenum Press, 1986).

[20] M. Sigalas, D. A. Papaconstantopoulos and N. C. Bacalis, Phys. Rev. B, **45**, 5777 (1992).

[21] O. K. Andersen, Phys. Rev. B, **12**, 3060 (1975).

[22] S. H. Wei and H. Krakauer, Phys. Rev. Lett., **55**, 1200 (1985).

[23] L. Hedin and B. I. Lundqvist, J. Phys. C **4**, 2064 (1971).

[24] J. J. More, in *Numerical Analysis*, G.A. Watson, ed., (Springer-Verlag, 1977).

[25] G. Simmons and H. Wang, *Single Crystal Elastic Constants and Calculated Aggregate Properties: A Handbook*, 2nd Edition, (MIT Press, Cambridge, MA, 1971).

[26] M.J. Mehl and D.A. Papaconstantopoulos, Europhysics Letters **31**, 537 (1995).

[27] C. Kittel, *Introduction to Solid State Physics*, (John Wiley & Sons, New York, 1971).

[28] J. Donohue, *The Structures of the Elements*, (John Wiley & Sons, New York, 1974), pp. 191-199.

[29] E. C. Bain, Trans. AIME **70**, 25 (1924).

[30] E. A. Brandes, ed., *Smithells Metals Reference Book*, 6th Edition, (Butterworths, London, Boston, 1983).

[31] F. H. Featherstone and J. R. Neighbors, Phys. Rev. **130**, 1324 (1963).

[32] A. F. Voter, "The Embedded Atom Method," in *Intermetallic Compounds: Principles and Applications*, ed. J. H. Westbrook and R. L. Fleischer (London: John Wiley & Sons Ltd., 1994), Vol. 1.

[33] M. I. Baskes, Phys. Rev. B **46**, 2727 (1992).

[34] M. J. Mehl and B. M. Klein, Physica B, **172**, 211 (1991).

[35] P. H. Dederichs, T. Hoshino, B. Drittler, K. Abraham, and R. Zeller, Physica B **172**, 203 (1991).

[36] H. M. Polatoglou, M. Methfessel, and M. Scheffler, Phys. Rev. B **48**, 1877 (1993).

[37] H.-E. Schaefer, Phys. Stat. Sol. (a) **102**, 47 (1987).

[38] F. R. de Boer, R. Boom, W. C. M. Mattens, A. R. Miedema, and A. K. Niessen, *Cohesion in Metals* Vol. 1 (North-Holland, Amsterdam, 1988).

[39] W. R. Tyson and W. A. Miller, Surf. Sci. **62**, 267 (1977).

[40] E. Cordwell and D. Hull, Philos. Mag **19**, 951 (1969).

[41] D. Tománek, Z. Sun, and S. G. Louie, Phys. Rev. B **43**, 4699 (1991).

[42] M. Methfessel, D. Hennig, and M. Scheffler, Phys. Rev. B **46**, 4816 (1992).

[43] M. Weinert, R. E. Watson, J. W. Davenport, and G. W. Fernando, Phys. Rev. B **39**, 12585 (1989).

[44] D. Singh, S.-H. Wei, and H. Krakauer, Phys. Rev. Lett. **57**, 3292 (1986).

[45] S. M. Foiles, M. I. Baskes, and M. S. Daw., Phys. Rev. B **33**, 7983 (1986).

[46] A. M. Guellil and J. B. Adams, J. Mater. Res. **7**, 639 (1992).

[47] W. R. Tyson, Can. Metallurgical Quarterly **14**, 307 (1975).

[48] D. A. Papaconstantopoulos and M. J. Mehl, Mat. Res. Soc. Symp. Proc. **408**, (1996) to appear.